BIOPHOTONIC APPLICATIONS OF ULTRAFAST FIBER LASERS: FROM BIOMATERIAL SURFACE MODIFICATION TO SUB-CELLULAR NANOSURGERY

A DISSERTATION SUBMITTED TO
THE DEPARTMENT OF MATERIALS SCIENCE AND
NANOTECHNOLOGY PROGRAM
AND THE GRADUATE SCHOOL OF ENGINEERING AND SCIENCE
OF BILKENT UNIVERSITY
IN PARTIAL FULFILLMENT OF THE REQUIREMENTS
FOR THE DEGREE OF
DOCTOR OF PHILOSOPHY

By
Mutlu Erdoğan
September, 2014

I certify that I have read this thesis and that in my opinion it is fully adequate, in scope and in quality, as a dissertation for the degree of Doctor of Philosophy.

Assoc. Prof. Dr. Fatih Ömer İlday (Advisor)

I certify that I have read this thesis and that in my opinion it is fully adequate, in scope and in quality, as a dissertation for the degree of Doctor of Philosophy.

Prof. Dr. Tayfun Özçelik

I certify that I have read this thesis and that in my opinion it is fully adequate, in scope and in quality, as a dissertation for the degree of Doctor of Philosophy.

Assoc. Prof. Dr. Sreeparna Banerjee

I certify that I have read this thesis and that in my opinion it is fully adequate, in scope and in quality, as a dissertation for the degree of Doctor of Philosophy.

Assist. Prof. Dr. Giovanni Volpe

I certify that I have read this thesis and that in my opinion it is fully adequate, in scope and in quality, as a dissertation for the degree of Doctor of Philosophy.

Assist. Prof. Dr. Doruk Engin

Approved for the Graduate School of Engineering and Science

Prof. Dr. Levent Onural
Director of the Graduate School

ABSTRACT

BIOPHOTONIC APPLICATIONS OF ULTRAFAST FIBER LASERS: FROM BIOMATERIAL SURFACE MODIFICATION TO SUB-CELLULAR NANOSURGERY

Mutlu Erdoğan
PhD in Materials Science and Nanotechnology Program
Supervisor: Assoc. Prof. Dr. Fatih Ömer İlday
September, 2014

Just a year after the invention of the LASER in 1960, it was demonstrated that lasers could be used for the treatment of certain skin abnormalities. At present, lasers are extensively used in a broad range of medical treatments.

After the development of femtosecond pulse lasers in the 1980s, even more exciting possibilities in a diverse range of fields have been realized. Accordingly, ultrashort pulse lasers are widely used in biological applications in recent years.

In parallel to these, fiber laser systems have increasingly been utilized in a wide range of scientific and biomedical applications, since they are highly compatible systems for being employed for industrial and biomedical applications.

Consequently, the aim of this Ph.D. thesis proposal is to develop compact, simpler to operate, and cost-efficient ultrafast fiber lasers with different repetition rates and pulse energies. By using such systems, we demonstrate the biophotonic applications of these lasers on two different biological research fields.

As a part of this thesis study, we develop ultrafast fiber lasers and apply them in biomaterial surface modification. We demonstrate that different surfaces with micro- and nano-scale topographies can be generated at high speed, precision and repeatability. The outcomes of biomaterial surface modification with different laser parameters are compared in terms of topographical uniformity and repeatability. Additionally, a variety of topographical modifications are assessed with respect to the efficiency on cell attachment and proliferation on metal implants.

As the second part of this thesis, we develop a custom-built ultrafast fiber laser-integrated microscope system for nanosurgery and tissue ablation experiments. Subsequently, we employ this system in order to make high-precision cuts onto different biological specimens ranging from the tissue level to subcellular level, such as a part of an axon or a single organelle. Finally, we improve this integrated system in a way that it becomes capable of generating optical pulses in any desired sequence possible. This is achieved by using acousto-optic modulators (AOM) and custom-developed field-programmable gate arrays (FPGA).

Keywords: Biophotonics, Nanosurgery, Tissue Ablation, Multiphoton Ablation, Ultrafast Laser, Ultrashort Pulse Laser, Fiber Laser, Biomaterial, Surface Modification, Implant Modification.

ÖZET

ULTRAHIZLI FİBER LAZERLERİN BİYOFOTONİK UYGULAMALARI: BİYOMALZEME YÜZEY MODİFİKASYONUNDAN HÜCRE-ALTI NANOCERRAHİYE

Mutlu Erdoğan
Malzeme Bilimi ve Nanoteknoloji, Doktora
Tez Yöneticisi: Doç. Dr. Fatih Ömer İlday
Eylül, 2014

LASER olgusunun 1960'taki keşfinden sadece bir yıl sonra, derideki bazı anormal yapıların bu teknoloji kullanılarak yok edilebileceği gösterildi. Günümüzde lazerler, tıbbi uygulamalar anlamında çok geniş bir kullanım alanı bulmuşlardır.

Buna ek olarak, 1980'lerde femtosaniye lazerlerin icat edilmesiyle birlikte lazerlerin daha birçok farklı alanda kullanılabileceği fark edilmiştir. Nitekim, ultrakısa atımlı lazerler, biyolojik ve biyomedikal araştırmalarda kendilerine her geçen gün daha fazla uygulama alanı bulmaktadır.

Tüm bunlara paralel olarak fiber lazerler, endüstriyel ve biyomedikal uygulamalardaki ihtiyaçlara son derece uygun oldukları için, bu alanlarda geniş çapta bir kullanım alan bulmuştur.

Tüm bunlar göz önüne alındığında, sunulan bu doktora tezinin hedefi; çeşitli tekrar sıklıklarına ve atım enerjilerine sahip olan, küçük hacimli, kullanımı basit ve düşük maliyetli ultrahızlı fiber lazerler geliştirmek ve bu sistemlerin farklı biyofotonik araştırma alanlarındaki uygulanabilirliklerini deneysel olarak göstermektir.

Bu bağlamda, bu doktora tez alışmasının bir bölümünde, farklı optik parametrelere sahip ultrahızlı fiber lazerler geliştirilmiş ve bu lazerler biyomalzeme yüzeylerini modifiye etmek üzere kullanılmştır. Ayrıca, mikro ve nano ölçeklerde topografilere sahip farklı yüzeylerin yüksek hızda ve hassaslıkta üretilebildiği de tarafımzca gösterilmiştir. Farklı lazer parametreleriyle modifiye edilmiş farklı yüzey yapıları, topografik düzgünlük ve tekrarlanabilirlik açısından

karşılaştırılmıştır. Buna ek olarak çeşitli topografik yapılar, hücrelerin metal implantlara tutunmasının etkinliği bakımından değerlendirilmiştir.

Sunulan bu tezin ikinci kısmında ise, doku kesimlenmesi ve nanocerrahi deneylerinde kullanılmak üzere bütünleşik bir ultrahızlı fiber lazer-mikroskop sistemi geliştirilmiştir. Bu sistem kullanılarak doku seviyesinde ve hatta tek bir akson veya tek bir organel gibi hücre-altı seviyelerde, yüksek hassaslıkta kesimler yapılmştır. En son aşamada bu bütünleşik sistem, optik atımları istenilen her şekilde üretebilecek ve örneğe gönderebilecek şekilde geliştirilmiştir. Bu amaçla, akusto-optik modülatörler (AOM) kullanılmış ve bu AOM'ler yine kendi geliştirdiğimiz alan-programlı kapı dizileri (FPGA) ile kontrol edilmiştir.

Anahtar sözcükler: Biyofotonik, Nanocerrahi, Doku Kesimleme, Çok-fotonlu Kesimleme, Ultrahızlı Lazer, Ultrakısa Atımlı Lazer, Fiber Lazer, Biyomalzeme, Yüzey İşleme, İmplant Modifikasyonu.

Acknowledgement

I am deeply grateful to my advisor F. Ömer İlday for his endless support, encouragement and confidence in me. His scientific enthusiasm inspired me to study in this field. I have always felt his encouragement and support that guides me to become an individual scientist, for which I will always be thankful to him. Moreover, I have also learned a lot from his communication and presentation ingenuities.

I also thank my friends and colleagues from UFOLAB. I especially want to thank Levent Budunoğlu for the stimulating discussions we have. I would also like to thank Seydi Yavaş for his long-standing friendship and his collaboration.

I want to specially thank my friends and colleagues, Volkan Ergin and Ergin Şahin, for the motivating and inspiring discussions and for their scientific collaboration.

I had the opportunity to work with Uygar Tazebay and I am grateful for his guidance and befriending. I also want to thank past Tazebay Group, especially Pelin Telkoparan, Elif Yaman, Hani Al-Otaibi and Defne Bayik.

The financial support from TÜBITAK and Bilkent University are also thankfully acknowledged.

Last but not the least; I would like to thank my parents Hüsran and Hakkı Erdoğan in addition to my sister Ceren Erdoğan for their support during my education.

Finally, I would like to give my special thanks to my beloved wife Emel, for her unending patience and support during this hard and tiring period and for here eternal love.

Mutlu Erdoğan,

September, 2014

Dedicated to my lovely wife, Emel...

Contents

List of Figures

List of Tables

Chapter 1

Introduction

The term biophotonics refers to the combination of biology and photonics, with photonics being the science and technology of generation and detection of photons in order to probe and manipulate biological phenomena. Biophotonics can also be explained as the "development and application of optical methodologies, especially imaging, to study biological processes in cells and tissues". One of the key advantages of using optical techniques for biology is that they are much less invasive compared to mechanical techniques, so that they highly preserve the biological integrity during examination. Thus, biophotonics has become the common term for all methodologies that contend with the interaction between biological substances and light.

1.1 History of Biophotonics

One of the earliest application fields of biophotonics is optical microscopy. Moreover, given that a greater number of organisms are not visible to the naked human eye, microscopy is probably the most important among all the techniques used in biology.

Today, microscope is undoubtedly the most fundamental element of biophotonics research. Like many other inventions there is a debate in origins of the inventors of the microscope. The same dispute applies to who invented the microscope. During the late 16th century, Dutch spectacle makers were experimenting with lenses and by putting numerous lenses in a tube, they made an important discovery: The size of the view of the object near the end of the tube appeared to be increased. Although this invention of the compound lens system paves the way for the observation of small organisms and cells per se, it was Anton van Leeuwenhoek (1632-1723), again a Dutch scientist, who in the late 17th century became the first man to make and use a real microscope. Van Leeuwenhoek was the first to discover and define microorganisms, which he originally reported as animalcules. Van Leewenhoek's work was verified and further developed by English scientist Robert Hooke, who published the first work of microscopic studies by collating them in the historical book *Micrographia*, in 1665. Robert Hooke's detailed studies opened up the scientific field of microbiology, and advanced biological science as a whole. He is also notable for coining the biological term *cell*; Figure 1.1.

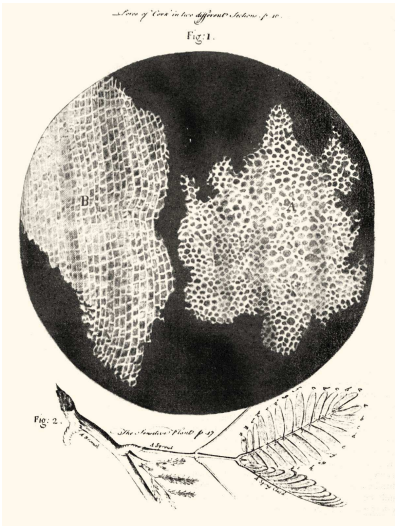

Figure 1.1: Hooke was the first person who described the cell. He applied the term *cell*, because plant cells, which are walled, reminded him of the cells in a honeycomb. *R.H., Micrographia, 1665.*

In the late 19th century, Koehler illumination, which is a method of specimen illumination that permits to generate an even illumination of the sample and that eliminates the formation of the image of the illumination source in the resulting image, was invented. Further inventions such as Phase Contrast by Frits Zernike and Nomarski Interference Contrast (DIC) by Georges Nomarski in mid-1900s, allow imaging of unstained, transparent samples. With these improvements in illumination and contrast-enhancing optical techniques, the microscope as we know it today has come into being.

In parallel to these later advancements in light microscopy, ideas on LASER concept began to emerge in early 20th century. Albert Einstein is one of the pioneers who studied the fundamentals of the nature of the light-matter interaction and established the theoretical foundations for the laser via a re-derivation of Max Planck's law of radiation, basically constructed on probability coefficients for absorption, spontaneous emission, and stimulated emission of electromagnetic radiation. Later in 1950s, Alfred Kastler proposed a technique for optical pumping, which was experimentally approved two years later, by Kastler, Brossel and Winter. Shortly after the first experimental demonstration of an optical or light laser in 1960s, biophotonics methodologies have been employed from ophthalmology to cosmetic surgery.

Ancient Greeks and Egyptians used sunlight for treatment, and even there is a mythological connection of such an idea that Apollo, the Greek god that is responsible for both healing and light. Although the idea of using light for curing illness has been recognized for thousands of years, it has only been since the invention of the laser in 20th century, which has revealed the potential of light for medicinal and biological purposes. The exceptional features of lasers make them much suitable than sunlight or other light sources for biological applications. Lasers operate within a specific narrow wavelength range and the light emitted is coherent, together with their capacity of reaching high optical powers. Their beams can be focused to very small points, which also enables high optical power densities. Such features have led lasers being utilized in a wide range of biomedical and biological research, e.g. Laser Scanning Confocal Microscopy and Laser Surgery are two of the most recognized examples of lasers contribution into

such research fields.

Discovery of the lasers has revolutionized biology and medicine. Especially with the demonstration of femtosecond lasers in the 1980s, investigators from a wide variety of research fields have acquired a versatile tool for probing and manipulating diverse range of natural phenomena. What makes ultrafast lasers particularly useful for biological and medical research is that they mostly operate in near infrared wavelength, which has a high penetration depth in biological tissue. Additionally, their ultrashort pulse duration makes it possible to reach high peak powers at very low pulse energies and average optical powers. For instance, an ideal laser system can generate 1 Joule of energy with 20 femtosecond pulses and the peak fluence value at the focal point can exceed 10^{20} W cm^{-3}, this is orders of magnitude higher when compared to the total solar flux at the Earth, which is approximately 10^{17} W.

An important advantage of ultrashort pulse lasers is that they enable time-resolved experiments with which ultrafast phenomena can be probed. Another biophotonic application in which ultrashort pulse lasers are utilized is multiphoton imaging of biological materials. In multiphoton microscopy, a fluorescent dye is excited through nonlinear absorption in a volume that is strictly limited to the focus of the objective lens, which permits for optical 3D sectioning as shown in Figure 1.2.

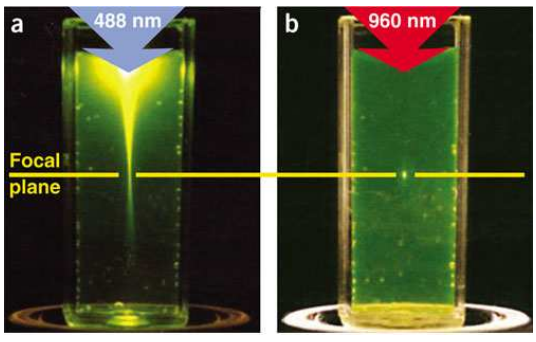

Figure 1.2: (a) Linear excitation of fluorescein dye by focused 488nm light. (b) Nonlinear excitation by focused fs pulses of 960nm light. [1]

An alternative and unique application of ultrashort pulse lasers takes advantage of the potential of these lasers on reaching enormous peak powers with moderate energies and optical powers. Through nonlinear interactions, ultrashort pulses are able to produce highly localized effects in materials. Hence, this makes ultrashort pulses especially suitable for ablation of biological materials, fragmentation (e.g. DNA into fragments that may be analyzed via Mass Spectroscopy), etc. In addition to these, another recent application field is ultrashort pulse laser micromachining of materials. Such ultrashort pulses are expected to result in cleaner cuts, because ultrashort pulse durations do not let the temperature to increase up at the irradiated area.

In parallel to all these advancements in optics and photonics, fiber laser systems have increasingly been utilized in a wide range of scientific and biomedical applications. Compatibility of a system for being used outside the research laboratory is a fundamental requirement for industrial and biomedical applications. Fiber lasers are clearly advantageous in this respect. In addition to their long-term stability in operation, the optical fibers provide isolated paths for light propagation, which minimizes the effects from the environment that may cause optomechanical misalignments throughout the system.

1.2 Future of Biophotonics: Nanobiophotonics

Nanobiophotonics is the next step of photonics in biological and biomedical applications. This step will literally be a small (*nano*) one, but will be a giant leap for mankind. The fantastic, though inevitable, combination of nanotechnology and biophotonics offers a great potential especially for the delivery of light in an extremely specific and controlled manner into living systems, together with the capability collection of data at the same precision.

A fictional, yet probable, world in which light-emitting and image-capturing nanorobots capable of navigating through tissues of organisms would be the culminant therapeutic technology for most of the diseases that the humankind has

encountered so far. In a state-of-the-art case, these nanorobots would circulate throughout the body with specific purposes, e.g. for detecting and counteracting cancer cells or for ultrahigh-resolution mapping of the neuronal networks in the brain as illustrated in Figure 1.3. Although such practices, at least for now, appear to be the subjects of far-future technologies, the integration of nanotechnology and nanophotonics into biological applications has already begun, so that novel terms such as nanobiotechnology and nanobiophotonics has emerged.

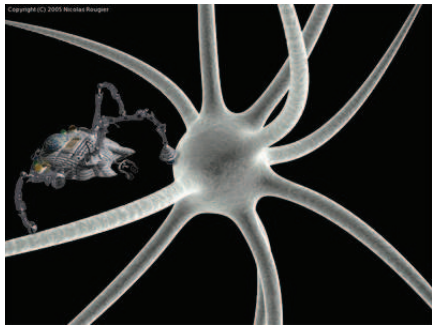

Figure 1.3: An artist's impression of a nanorobot in the vicinity of a neuron [2]

The ideal integration of photonics into nanobiotechnology and thereby the technological achievements imagined are fundamentally dependent on the advancements in nanophotonics. Nanophotonics is a field that investigates the behaviour of light on the nanometer scale, conceptually on a scale much smaller compared to the wavelength of light used, and of the interaction of nanometer-scale objects with light [3]. In order for this integration to occur as envisioned, nanoscale confinement in different methodologies of photonics must be achieved, and these can basically be categorized as *nanoscale confinement of radiation*, *nanoscale confinement of matter* and *nanoscale photoprocesses* [4].

Today, nanoscale confinement of radiation is conceptually the subject of near-field optics, a branch of optics that deals with exceeding the optical resolution limit (mainly diffraction limit) by engineering the properties of evanescent waves. Contemporarily, near-field optics and microscopy has emerged as a powerful biological research methodology to observe submicron-sized biological structures and to probe functions of nanoscale phenomena.

The optical resolution limit of conventional microscopes, that is diffraction limit, is approx. half the wavelength of the illumination light. Thereby, while imaging at visible spectrum, the minimum resolvable structures are in the order of hundred nanometers. In contrast, by exploiting near-field optical methods, it has been achieved to optically resolve structures as small as a couple of tens of nanometers in size. At this point, it is important to note that the most widely employed near-field apparatuses as near-field probes are tapered optical fibers. The light, either delivered or collected, propagating through the fiber leads to a resolution determined by the dimensions of the tip of the fiber and its distance from the specimen. The size of the fiber tip is usually around a few tens of nanometers and the resolution of a near-field system is mainly dependent on the probe size, thus, such factors necessitates further developments in nanoscale confinement of matter in terms of producing nanometer-sized probes and light sources.

Nanoscale confinement of matter considering nanophotonic applications exploits the nanoscale manipulation of molecular architecture and anatomy, which allows to precise control over the optical and electronic properties of a material. For instance, if light can be transmitted in a confined manner, it can also be detected with a confined detector. In parallel to these, researches that deal with reducing the sizes of light sources such as lasers and LEDs into nanometer scale will result is an the development of ultra-compact light emitters exhibiting both optical and electrical functionalities. Such technological innovations require a priori knowledge and a better understanding of fundamentals of nanophotonics; thus, contemporary sciences of optics and photonics are now at this phase. Two interesting examples are generation of light with nanolasers [5] and nonlinear plasmonics [6]. The initial applications of the technological achievements in nanophotonics would likely be into the data transmission and communication systems, but as happened previously in the invention of the lasers and their employement in biological applications, it will not take much time to convert the methodologies of nanophotonics into tools of nanobiophotonics.

Nanoscale photoprocesses such as optical lithography offer facilities for nanofabrication. For instance, near-field photolithography can be employed for

creating nanometer scale chip-arrays for nucleic acid detection. Such nanometer-scale photoprocesses enables the production of ultra-high density chip-arrays, thereby allowing the use of lower quantities of specimens. This holds an excellent potential for analysis of biochemicals with minuscule amounts, e.g. even at the nucleic acid levels for which there is no possibility of PCR amplification that enables detection. Such a methodology will allow to earlier diagnosis of diseases when compared to current molecular and biochemical diagnosis technologies, even at the moment of infection.

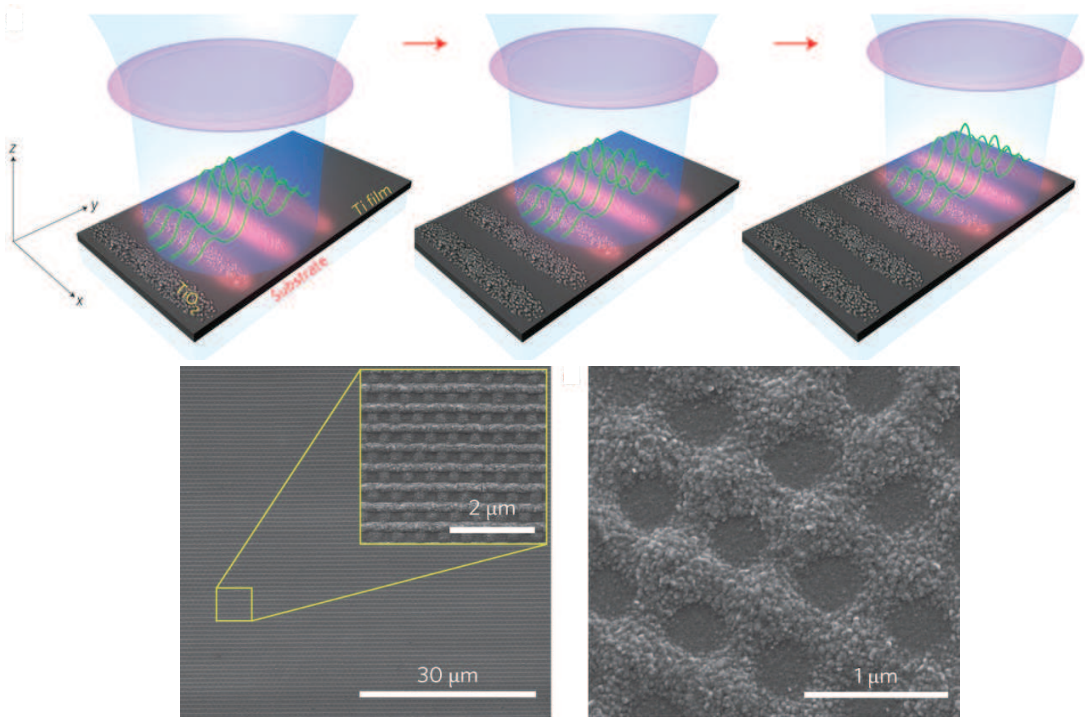

Figure 1.4: (Upper panel) Schematic of the nanofabrication process when while the laser beam is scanned over the surface. (Lower panel) SEM image of mesh nanostructures -left- and nanocircles -right-. [7]

Thus, micro- and nanofabrication on surfaces is increasingly becoming important and widespread in nanotechnology researches. There are already established methods such as e-beam lithography, photolithography and interference lithography. Recent developments such as the demonstration of a technique that utilizes nonlocal feedback mechanisms for ultrashort pulse laser-induced nanostructuring

with extreme uniformity and speed, even on non-planar surfaces, is especially exciting and promising [7]. The capability of the methodology allowing structuring of indefinitely large areas even at sub-nanometer precision, as shown in Figure 1.4, is particularly promising for nanophotonic, plasmonic, photon detection, nanoelectronic applications and especially for engineering superior quality biomaterial surfaces for the manipulation and control of cell behaviours in nanometer precision.

1.3 Overview of the Thesis

Considering all these, as a part of this thesis study, we develop ultrashort pulse fiber lasers and demonstrate their use in biomaterial processing. We demonstrate that different surface topographies with micro- and nano-scale features can be generated at high speed, precision and repeatability. The outcomes of biomaterial surface modification with alternative laser parameters are compared in terms of topographical uniformity and repeatability. Additionally, the results of various different surface modifications are evaluated with respect to the efficiency of cell attachment and proliferation on the medical implants.

As the second part of this thesis, we develop a custom-built ultrafast fiber laser-based microscope system for nanosurgery and tissue ablation experiments. Furthermore, we applied this system for doing high-precision cuts, to various biological specimens ranging from the tissue level to subcellular level, such as a part of an axon or a single organelle. Finally, we improve this integrated system such that, through the use of AOM's and custom-developed FPGA's, it can generate arbitrary pulse patterns with no limitations.

Chapter 2

Biomaterial Surface Modification

Biomaterial is a term that specifies any substance that has been engineered to take a form, and alone or as part of a composite system, to regulate the progress of any therapeutic or diagnostic procedure, by controlling the interactions between the constituents of living systems. During these procedures, the main part of the biomaterial that directly contacts with the living system is the surface of the biomaterial. Hence, biomaterial surface modification have an important role in manipulating the interactions between the biomaterials and living systems. Through appropriate modifications of their surfaces, biomaterials can be altered to improve biocompatibility, attachment and tissue interactions. Thus, surface modification is critical in the design and development of novel biomaterials and medical apparatuses. Thereby, modification of biomaterial surfaces aims to enhance biological performance by optimizing the interactions within the living system.

2.1 Theoretical Background of Biomaterial-Tissue Interaction

The subject of biomaterials embodies the combination of physical and biological sciences. As a matter of course, it is of great consequence that these aspects are combined to develop eligible biomaterials that function optimally in biological environment. The key to this issue remains in the interactions between the biological substance of interest and biomaterials . The recent scientific and technological advances in fields such as molecular and cellular biology, biotechnology and tissue engineering as in other connected disciplines, gave rise to an importortant increase in the development and utilization of apparatuses with bio-logical/-medical purposes, such as catheters [8], heart valves [9], and scaffolds for tissue engineering [10, 11]. Nevertheless, mainly because of the fact that an implanted biomaterial naturally undergoes a functionality loss through time after implantation, it is critical to establish an effective and mechanically stable integration of the biomaterial to the surrounding tissue. Inadequate in vivo functionality and permanency of this integration are essential issues, originating either from the normal homeostatic or the abnormal reactions against the implantation, or even to the lack of biocompatibility per se, between the biomaterial and the living system [12, 13, 14].

There are many factors having a role in the efficiency of the biomaterial used as an implant, and being influential on the fate of the implant in the living system. In addition to the physical and mechanical features of biomaterials, the core and determinative factor is the interaction between the biomaterial and the surrounding tissue. These interactions are predictable only to some extent due to their complex nature and comprise many factors, elements and elaborate interactions; yet, a brief but practical categorization has been made by D.F. Williams, considering the essential phases of the integration of a biomaterial to a living system [12]:

(1) "The initial events that take place at the interface, largely concerned with the physicochemical phenomena that take place in times measured in seconds or

minutes following contact between biomaterial and tissues;

(2) "the effect that the presence of a foreign body has on the tissue surrounding the implant, which may be seen at any time ranging from minutes to years;

(3) "the changes seen in the material as a result of its presence in the tissues, usually described under the headings of corrosion or degradation; and

(4) "the sequelae of the interfacial reaction that are seen systemically (that is, throughout the body) or at some specific but remote site.

These events cooperatively outline the biocompatibility phenomenon.

One of the fundamental concerns in biomaterials studies is biocompatibility. In brief, biocompatibility is general a term for the nature and the status of interaction between biomaterials and living systems [15, 16]. Given that the response to different materials could also differ from one application to another, biocompatibility could not only be dependent on the properties of material itself, but also has to be related to the situation in which the biomaterial is employed. Moreover, an increasing number of studies demonstrated that the biomaterial should respond to the tissues in concordance with the planned application, rather than be ignored by them [17]. In relation to this, it is necessary for some applications that the biomaterial should decompose or degrade over time in the body, rather than staying indefinitely. Hence, a more accurate and appropriate definition would be:

"Biocompatibility is the ability of a material to perform with an appropriate host response in a specific situation [17].

It seems that there are numerous distinct ways in which biomaterials and living systems interact with each other so that it is usually challenging to unravel the underlying mechanisms. Collection of information and comprehension of these interactions is essential for designing of biomaterials that give the optimized performance and these are primarily evaluated in the broad context of the biocompatibility phenomenon.

The introduction of a foreign substance into living tissue on purpose such

as a medical implant used in biomedical applications, or by mistake as when a splinter penetrates into the tissue gives rise to the formation of interfaces between the material and the surrounding tissue. In terms of the kinetics and thermodynamics, surfaces have different characteristics compared to corresponding bulk of the material and contain reactive bonds, which in turn lead to the formation of surface reactive layers such as the surface oxide layers on metals [18, 19]. Meeting with the living system precedes surface reactions that alters the surface, and causes to the adsorption of water, ions, and biomolecules, which are in a dynamic equilibrium within the living system. Interruption of the exact nature of these dynamics influences the behaviour of cells connecting the material surface, and hence the tissue response.

The surface of a material is a termination of a three-dimensional structure, and therefore, as a rule, corresponds to an increase in energy; at the atomic level, this energy is represented as unsaturated bonds and if there is a reactive environment as in air or water meets a metal surface, these terminals readily react to create new bonds and compounds, thus lowers its surface energy [19]. In parallel to these, living systems consist of a mixture of biomolecules such as water, oxygen, cations, anions, proteins etc. The biological and non-biological substances contact and interact at the interface, which might react to lower the surface energy of the system. There are two key factors that disable such undesired reactions; one of which is that when the material and the living system are disconnected, both substances have their lowest thermodynamic state already, and the other factor is that the inherent kinetic barriers prevent all possible reactions [19, 20].

The chemical components of the biological milieu effect the interactions at the interface [19, 20]. For instance, in case the biomaterial is metal-based, corrosion may cause the release of metal ions from the metal-oxide surface into the milieu within the biological system, which has a potential for triggering adverse systemic effects [21, 22]. In addition to this, a biomolecule at the biological side of the interface and the biomaterial surface at the other side may form momentary van der Waals bonds or even covalent bonds, which are stronger and stable. In case that such interactions are so strong, macromolecules may irreversibly become denatured [23].

In the medium and long term, the larger and more complex elements like cells communicate the interface with their membrane. In view of the fact that the cell membrane as a composite bioorganic structure and the biomaterial surface are both active, they may develop a complex and dynamic interface. Depending on the properties of the surface of the material, cells respond differently to different biomaterials.

Eventually, the ultimate aim of engineering the tissue-biomaterial interface is to control cellular responses. The basic approach to this this phenomenon is to consider the factors those are used by cells when they are interaction with the surrounding substrate, and the parameters those are utilized by surface scientists when they are trying to control the interactions between different materials. Such factors or cues to which a cell will respond can principally be categorized into three categories: Chemical, topographical, and mechanical. These three different types of factors can have related effects [23]. It is recognized that the structure of a biomaterial surface rules the phenotypic response of interacting cells [24]. Accordingly, surface features such as chemical composition, hydrophobicity and roughness are all known to have influence on the response of cells that interact with a biomaterial. Moreover, there is an intertwined relationship between these diverse properties of a surface and altering one feature practically alters others as well. For instance, altering hydrophobicity of a polymer biomaterial is accompanied with a change in the chemical composition of side groups at the surface of the biomaterial, hence its surface energy [25, 26].

On the other hand, recent maturation of biological studies in parallel to the outcomes of the Human Genome Project, along with accompanying technological progresses in molecular and cellular biology, places the strategies and methodologies of molecular and cellular biology into a distinctive position. By being equipped with the capability of examining the gene/protein expression changes within biological systems of interest via transcriptomic and proteomic methodologies, molecular biology has led to further understanding of the molecular basis of a broad range of physiological activity at the biomaterial-tissue interface [27, 28].

In addition to the physicochemical properties of the surfaces of biomaterials,

cells also substantially interact with the topographical features on these surfaces, as shown in Figure 2.1, principally through a phenomenon known as contact guidance [29].

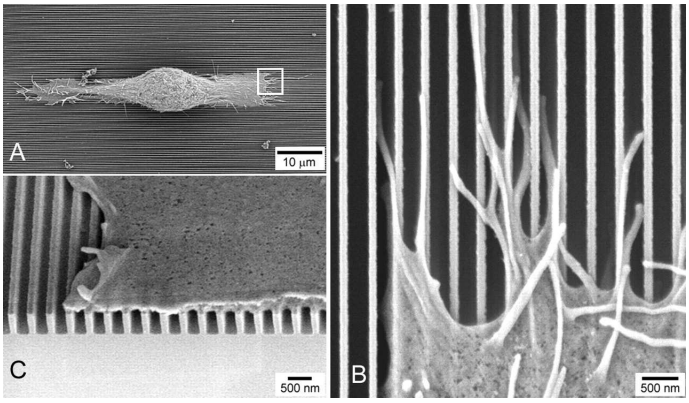

Figure 2.1: SEM images of cells cultured on nanostructured substrates. [30]

The topography of material surfaces regulates a range of cellular processes such as cell adhesion, cell shape and cellular differentiation [31]. For instance, epithelial cells attach and align along grooves and ridges with feature dimensions smaller than 100 nm [30]. Nanoscale topographic textures induce mineralization of human mesenchymal stem cells [32]. Another example to such topographical guidance behaviour is that human SaOS-2 osteosarcoma cells cultured on metal surfaces with parallel lines of different widths and distances often orientate along these parallel lines [33]. Besides, tissue-biomaterial interactions are also directly related to the fact that different cell types respond differently to alterations in the same surface property. For example, increasing surface hydrophobicity induces adhesion of endothelial and epithelial cells to the surface [26], but reduces adhesion of osteoblasts [34].

Consequently, a complete understanding of tissue-biomaterial interactions is the key parameter that will pave the way for designing and developing functional biomaterials and medical implants. And, because of the fact that the biomaterial surface is the major portion that directly interacts with the surrounding tissue, it is critical to have methodologies that allow the modification of surface properties

such as topography. Such methodologies would lead to development and costless production of higher quality medical implants with optimum performance.

2.2 Surface Modification of Medical Implants

Hard tissues are mineralized biological tissues that contain minerals in soft matrices. Usually these tissues provide a structural support or protective shield [35]. In addition to the mollusc shells, radiolarians, diatoms etc.; there are several mineralized tissue types, and so called hard tissues, such as bones, tooth enamel, dentin, tendons and cartilage found in the human body [35, 36].

On the other hand, bone is one of the few tissues in the human body that is capable of undergoing spontaneous regeneration and having a high capacity of remodeling its micro- and macro- structure. This is accomplished through a precise balance between the osteogenic (bone forming) and osteoclastic (bone removing) activities [37], which enables bone tissue to adapt to different mechanical environments by allowing it to adjust the dynamic balance between these two biological processes.

As hard tissue replacements have become an conceivable treatment for patients, it also has become even more evident that the interaction between host tissue and the implanted biomaterial surface is of critical importance. The whole biological response of host tissue to medical implants can be separated as two different, but interconnected periods. Initial period comprises the biological processes of a clinical healing, which immediately follows the implantation of the biomaterial. During this recovery period, the early biological activities and molecular deposition on the biomaterial surface are followed by cell adhesion, migration, and differentiation. It is thus crucial to realise the characteristics of the biomaterial, which have an influence on the initial formation of the host tissue-implant interface. These early tissue activities result into cellular expression and extracellular matrix formation and eventually into the development of bony interfaces with the implant [38]. With Branemarks and his colleagues huge amount of contribution

to this research field, the characteristics of the implant substrate which permit biomaterial-tissue integration has been realized. When the early healing period is completed, within months, the maturing interface transforms as biomechanical stresses are placed on the implant, and this also is closely interrelated to the initial degree of tissue-implant surface interaction [39].

At this point, osseointegration phenomenon becomes critical and determinative. The concept has been portrayed by Branemark as the direct contact between bone and implant, principally on the light microscopic level [40], as illustrated in Figure 2.2.

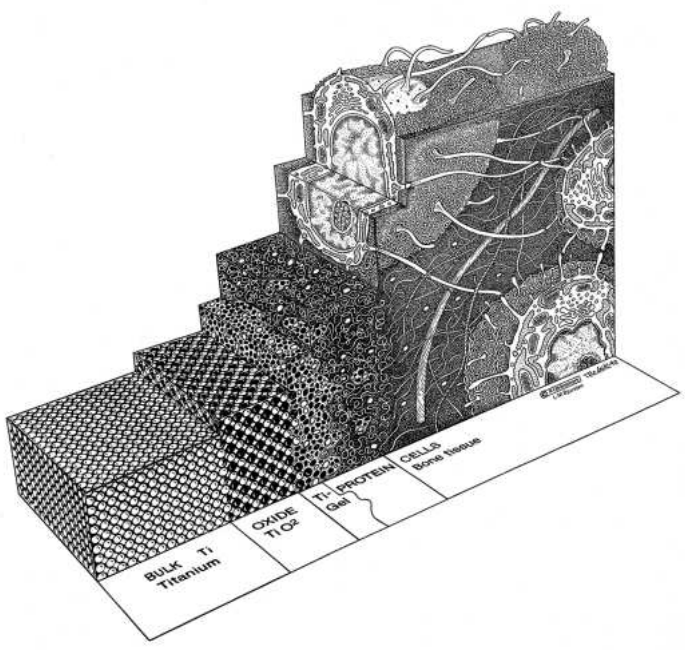

Figure 2.2: A representative picture of the implant/tissue interface. The surface of titanium is in contact with the living bone [39]

Currently, an implant is regarded as osseointegrated if there is no progressive relative movement between the implant and the bone with which it is directly contacted. During the osseointegration process, mesenchymal cells and osteoblasts migrate and attach to the surface of the biomaterial, beginning from the early stages of implantation. With the accumulation of bone-associated proteins and

establishment of a extracellular layer on the implant surface that controls cell attachment and mineralization, integration of the bone tissue and the biomaterial begins [41]. Subsequent to this, primary bone formation occurs on implants to reestablish continuity. Primary bone structure fills the initial space at the implant-bone boundary. The physical architecture of a three-dimensional regular network provides a biological scaffold for cell attachment and bone sedimentation, [42]. Eventually, bone in contact with the implant surface goes through morphological remodeling as adaptation to biomechanical stress and loading. During the remodeling of this peri-implant bone, new osteons circle around the implant perpendicular to the long axis of the implants. Osteoid tissue is generated by osteoblasts, which indicates that osteogenesis is in progress. A remodeled bone at its later stages can expand up to 1 mm from the implant surface [42].

Different materials and implant surface treatment together with surface coatings have been proposed to enhance the quality of osseointegration. The biocompatibility of the biomaterial is of great importance and a necessity for osseointegration. In this regard, titanium metal is widely used as a hard tissue replacement implant material. Titanium has significant advantages with its great biocompatibility, resistance to corrosion and lack of toxicity on living systems with its little, if any, inflammatory response in peri-implant tissues [43]. Titanium's low density [4.5 g/cm3] and good mechanochemical characteristics are main parameters for implant application. There are various types of commercially available titanium and titanium alloys for surgical implant applications. Ti6Al4V titanium alloy is extensively utilized to construct implants. The core alloying elements of the Ti6Al4V are aluminum (5.5 6.5%) and vanadium (3.5 4.5%). The addition of alloying elements to titanium allows it to gain a numerous features e.g. Aluminum and Vanadium serves for the resistance to the external forces and strengthens against mechanical loads [43].

Metal surface modification is frequently utilized for enhancing osseointegration by means of the manipulation of the dynamics at the tissue- biomaterial interface. Cells at the interface and their secreted biochemicals involved in the course of osseointegration change the organization and physiochemical features of the biomaterial surface. Interconnectedness in the case of macro-featured surfaces

and surface roughness in the case of micro-featured surfaces are generally considered as suitable surface structures for osseointegration [44]. Besides, surfaces of biomaterials are rarely smooth at the molecular level mostly due to the processes the fabrication of the biomaterial and these surface features, such as roughness may or may not be formed intentionally. On the other hand, micron-sized topography has been demonstrated to have a central role in regulating cell adhesion and tissue-biomaterial integration [45]. Biomaterial modifications are recently of particular interest, with the aim of controlling cell adhesion and spreading. In this regard, modification of biomaterial surfaces, particularly by considering the topographical surface properties, is at utmost importance [46]. There are various kinds of metal implant surface modification targeting topographical features such as titanium plasma spraying, hydroxyapatite coating, machine processing, polishing, sandblasting and acid etching. These techniques are among the most commonly used commercial surface modification methods [47].

On the other hand, these techniques commonly used to create surface textures in commercial applications are all incapable of creating selective and tailored-topography, which is recently of particular interest for the control of osseointegration in a precisely regulated manner. Recently, laser surface texturing has emerged as a novel technology for creating a large variety of micro- and even nano-structured biomaterials including medical implants. Laser texturing of material surfaces has exceptional advantages over other surface structuring techniques, e.g. photolithography, such as:

(1) Capability of modification of virtually all types of materials, including metals and polymers;

(2) Competence for texturing of non-planar surfaces;

(3) Capacity to create micro- or nano-structures on surface areas from micro-scale to macro-scale;

(4) Maskless single-step processing even at high speeds under normal environmental conditions, without the requirement of a clean room facility.

Although surface patterning can be performed using continuous lasers, nanosecond or longer-pulsed lasers, they lead to unwanted thermal effects, which is restrictive for the degree of precision. Thermophysical response of the material is dependent on the pulse length of the laser and shows substantial differences below and above the picosecond regime. Ultrashort pulses in the pico- and femtosecond regimes have significantly reduced thermal effects, enabling high-precision and confined processing with little or no effect to the incident region on the textured material surface [48].

In this regard, high precision can be achieved by employing ultrashort-pulsed solid-state lasers [49]. Nevertheless, they are complicated and costly devices; hence, application of them on surface modification of biomaterials has been restricted mostly to laboratory experiments. Ultrafast fiber lasers offer excellent potential for biomaterial surface modification at micro- and nanoscale with an exceptional spatial control. Operating at high speed and together with their desirable features such as robust operation, low cost, compact size, low intensity noise and diffraction-limited beam quality; modification of biomaterial surfaces using ultrafast fiber lasers is a promising methodology.

2.3 Experimental Methods

2.3.1 Sample Characterization

2.3.1.1 Scanning Electron Microscopy (SEM)

Micro- and nanostructural observations of the titanium surfaces are carried out using the scanning electron microscope in UNAM, Bilkent University; E-SEM, Quanta 200F, FEI on ultra-high resolution mode with ETD detector under ultralow vacuum conditions are used with approx. 10 kV. Imaging of cell attachment on titanium surfaces are performed with the same microscope by using GSED detector under low vacuum conditions without application of any conductive coatings in order to directly observe the morphologies, operated at approx.

5 kV.

2.3.1.2 Atomic Force Microscopy (AFM)

The surface topography of the titanium implants are analyzed using the atomic force microscope in UNAM, Bilkent University; AFM, XE-100E, PSIA in non-contact mode.

2.3.1.3 Energy-dispersive X-ray Spectroscopy (EDX)

The chemical structure of the modified areas are identified through EDX analyses. EDX analyses are performed using Bruker AXS detector with ultra-thin window attached to the Carl Zeiss Evo40 SEM in Dept. of Chemistry, Bilkent University.

2.3.1.4 Raman Spectroscopy

Further chemical structure analysis of the modified areas are carried out through the Raman spectroscopy in Dept. of Chemistry, Bilkent University. Horiba Jobin Yvon micro-Raman equipment is used for Raman analyses, where the source of radiation was a laser operating at a wavelength of 632.8 nm and a power of 25 mW.

2.3.1.5 Bright-field Optical Microscopy

Optical imaging of nanostructural textures is performed with the light microscope in UNAM, Bilkent University; Axio Scope.A1, Carl Zeiss at room temperature conditions.

2.3.2 Cell Culture

2.3.2.1 Cell lines and Growth conditions

Human osteosarcoma cell line SaOS-2 is used for cell attachment and proliferation. The cells are cultured in McCoys 5A medium supplemented with 15% fetal bovine serum, 2 mM L-glutamine, streptomycin/penicillin 100 U/mL, and in a humidified atmosphere of 95% air and 5% CO_2 at 37°C.

2.3.2.2 Attachment and Proliferation Assays

Cells are seeded onto 8-mm diameter Ti6Al4V disks with three different commercially-modified surfaces and different fiber laser-modified surfaces. Before use, all samples are sterilized for 30 minutes in 10% NaClO with an ultrasonic cleaner and placed in 24-well cell culture plates with a density of 100,000 cells/ml. Separate attachment tests are done for incubation periods of 36 hours and 7 days.

2.3.2.3 Fixation and Fluorescent Imaging of Cells Attached on Implants

At the end of the incubation periods, disks are washed with PBS, treated with trypsin/EDTA solution for 20 seconds to eliminate the poorly attached cells, and then fixed in 0.1 M sodium cacodylate buffer with 3% glutaraldehyde, pH 7.2 at 4°C overnight. For each surface type, 3 Ti disks are used (samples are triplicated), hence 12 Ti disks are used for each incubation period in total. Following up the fixation stage, cells are stained with 300 nM 4, 6-diamidino-2-phenylindole, dilactate (DAPI, dilactate) in PBS and with Mitotracker Red 580 (Invitrogen) in McCoys 5a and subsequently counted under a fluorescent microscope (Nikon Eclipse Ti/U).

2.3.2.4 Cryopreservation of Stock Cells

Exponentially growing cells in 100 mm cell culture plate were harvested by trypsinization and collected in 5 ml growth medium. Then, cells were precipitated at 1500 rpm for 3 min. The pellet was suspended in a freezing medium (8% DMSO, 92% FBS). Pellets were resuspended in 1 ml freezing medium in cryotubes and they were left at -20°C overnight. The next day cells were stored at -80°C for 1 day to 1 month. Finally, the tubes were transferred into the liquid nitrogen storage tank for future experiments.

2.3.2.5 Thawing of Frozen Cells

The frozen cell line was taken from the liquid nitrogen tank and immediately put on ice and then placed into a 37°C water bath for 1-2 minutes. The cells were transferred into 15 ml tubes and resuspended in 9 ml growth medium. The cells were centrifuged at 1500 rpm for 3 minutes. Supernatant was discarded and the pellet was resuspended in 10 ml culture medium to be plated into 100 mm dish. After overnight incubation culture mediums were replenished.

2.4 Results

2.4.1 Surface Modification with Pulsed Fiber Lasers

Biomaterial surface modification is currently of special interest, with the aim of directing cell attachment and spreading. In this context, modification of biomaterial surfaces, especially in consideration of the surface topographies, is at utmost importance [46]. There are different, commercial, metal implant surface modification types, focusing on the generation of discernible topographical features e.g. titanium plasma spraying, hydroxyapatite coating, machine processing, polishing, sandblasting and acid etching (For some examples, Figure 2.3).

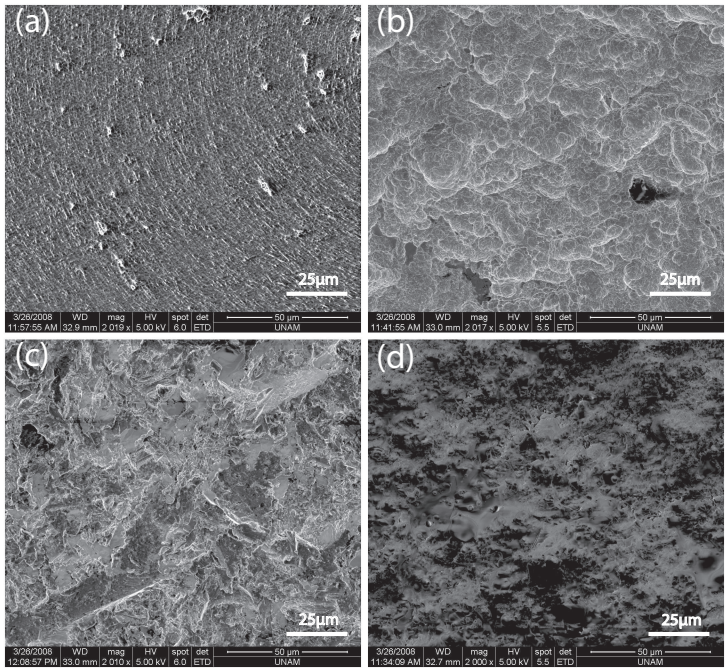

Figure 2.3: Examples of commercially-modified metal implant surfaces. (a) Acid etched, (b) SLA, (c) Sand-blasted (d) Hydroxy-apatite-coated (M.E. archive).

Although these techniques are among the most commonly-used commercial surface modification methods [47], they are all incapable of creating selective and tailored-topography, which is recently of particular interest for the control of osseointegration in a precisely controlled manner. On the other hand, laser-based surface modification has emerged as a novel methodology for generating a great diversity of micro- and even nano-structured biomaterial surfaces including medical implants.

Laser surface modification has been increasingly used as a novel methodology for creating precisely-controlled surface topopgrapies on biomaterials such as metal medical implants. Laser modification of biomaterial surfaces has significant advantages over other surface modification techniques such as being capable of modification of almost all types of materials, and of creating fine structures on surface areas from micro- to macro-scale (e.g. Figure 2.4).

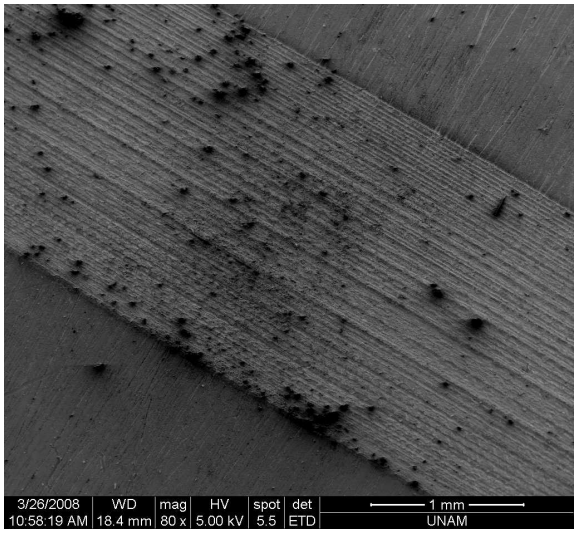

Figure 2.4: Titanium surface modified with the laser parameters of 3W output power, 80 ps pulse duration (M.E. archive).

For the purpose of surface modification, we develop and make use of short- and ultrashort pulse fiber lasers with MHz-repetition-rate, microjoule- and sub-microjoule-energy pulses [50]. Modification of Ti6Al4V alloy-based biomaterial surfaces is performed using home-built femtosecond and picosecond pulsed fiber lasers. Additionally, we make a comparison of the effects of these regimes with nanosecond regime by using a commercial nanosecond fiber laser.

We utilized home-built picosecond and femtosecond pulse fiber laser systems in order to assess the effects of MHz-level repetition rates and of relatively low pulse energies on biomaterial surface modification. We demonstrate that a range of surface topographies with micro- and nano-scale features can be created at high speed with high precision and repeatability. We compared the results of picosecond and femtosecond pulses with those of commercial nanosecond fiber laser and as a result, we showed that there are significant thermal effects with reduced precision in nanosecond regime. In the end, effects of various surface topographies on cell adhesion and proliferation is investigated.

The experimental setup is depicted in Figure 2.5. Two distinct, custom-built

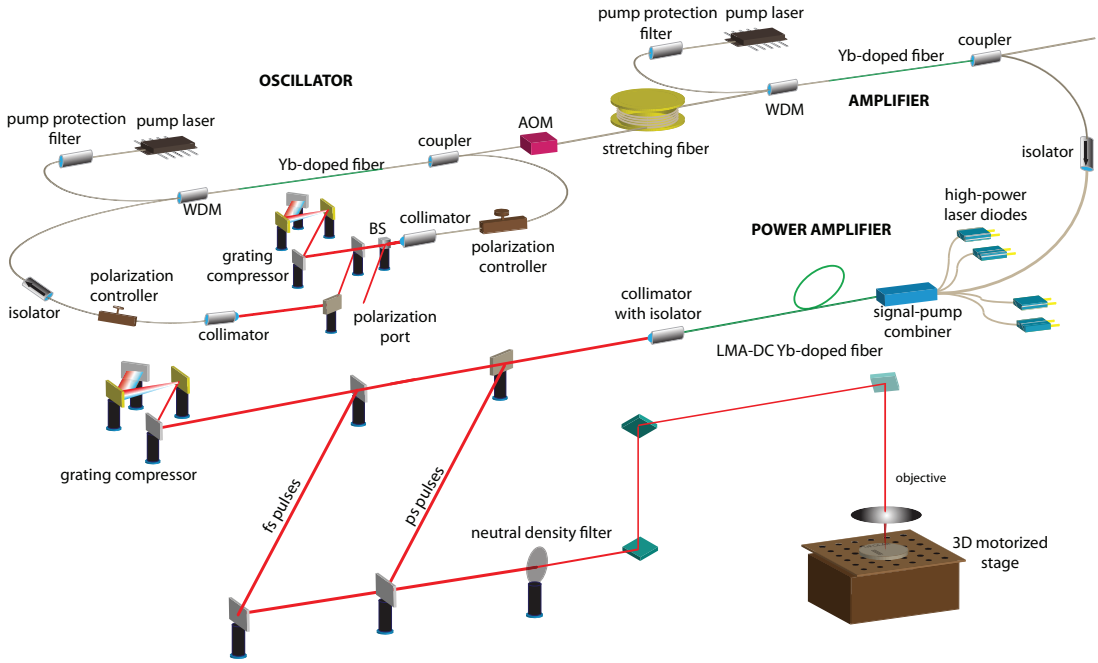

Figure 2.5: Depiction of the ultrashort pulsed all-fiber-integrated Yb amplifier and the biomaterial modification setup, BS: beam splitter, AOM: acousto-optic modulator, LMA: large mode area, DC: double-clad.

pico- and femtosecond fiber laser systems and a commercial nanosecond fiber laser (FL-NS-8W, FiberLAST) are utilized in this research. The nanosecond laser generates 70 ns-long pulses at 20-200 kHz repetition rate and maximum average optical power of 8 Watts.

One of the ultrashort pulse laser systems is seeded by an all-normal-dispersion (ANDi) mode-locked Yb oscillator [51] with a central wavelength of 1060 nm and the other one by a self-similar mode- locked Yb oscillator [52] with a central wavelength of 1035 nm. The oscillator repetition rates are 43 MHz and 28 MHz, respectively. Both oscillators produce few picosecond-long, chirped pulses, which are fiber-coupled to all-fiber-integrated and misalignment-free amplifiers. First, the pulses are temporally stretched in fiber stretchers to reduce nonlinear effects, then traverse preamplifiers, which boost the power to 100-150 mW, which is sufficient to seed the power amplifiers. Both systems incorporate 10 ns-risetime fiber-coupled acousto-optic modulators (AOM) to optionally reduce the repetition rate to 1 MHz prior to amplification. This first system generates an average power of up to 16 W, corresponding to an estimated peak power of 20 kW for 20 picosecond pulses at 43 MHz of repetition rate. Following pulse compression with the gratings, pulse duration is measured to be 200 femtosecond full-width at half-maximum (FWHM) [53].

The second system is utilized only at the lower repetition rate of 1 MHz in order to increase the pulse energy. The pulses are stretched to 150 picosecond in a 100-m long fiber stretcher and amplified to 104 nanojules in the preamplifier. The nonlinear chirped-pulse power amplifier generates pulses with up to 4 μJ energy at 1 MHz repetition rate. The pulse duration is reduced to 80 picosecond during amplification as a result of gain filtering clipping the edges of the pulse in the time domain. The maximum peak power of amplified pulses is 57 kW and the compressed pulse duration is 150-200 femtoseconds [54].

Both laser systems can operate in picosecond mode by simply bypassing the pulse compressor. When the compressed pulses are utilized, they are always linearly polarized due to the grating compressor. Uncompressed pulses can either be unpolarized or optionally linearly polarized with a polarizer.

For modification with the home-built ultrashort pulse fiber laser systems, the beam is focused to a focal diameter, changeable in the range of 10-15 μm using a high-power and 1 μm-wavelength-compatible microscope objective. The processing setup includes a collimator telescope, an objective and a 3-axis motorized and computer-controlled translation stage. Numerous surface textures can be generated by moving the translation stage on which the samples are located. For texturing with the commercial ns-pulsed fiber laser, the beam is scanned over the sample with a computer-controlled galvanoscanner, using a special objective designed to preserve a uniform spotsize irrespective of the deflection angle. The focal diameter in the focal plane is approximately $\sim$40 μm. All three laser systems have nearly diffraction-limited beam quality ($M^2 < 1.2$) and they can be switched off within microseconds for jumping from one point to another. Scan rates used in the experiments range between 3 μm/s and 50 μm/s.

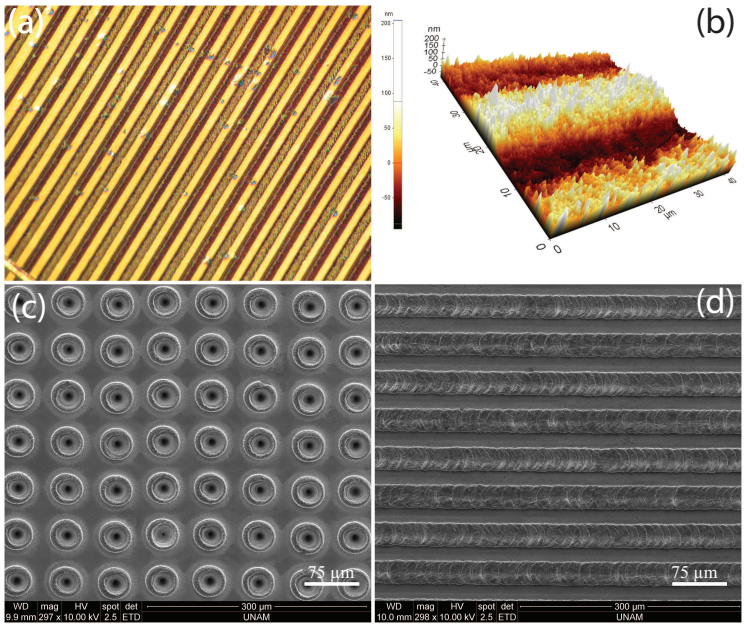

Figure 2.6: Various examples of surface modifications created by femto- and picosecond fiber lasers. Optical (a) and atomic force (b) microscope images of the nanoscale surface topographies. (c, d) SEM images of the microscale surface topographies.

By employing the systems mentioned above, we demonstrate that a great diversity of surface patterns can be generated using both the femto- and picosecond pulses by adjusting the pulse energy, duration, exposure time and the scanning texture. Samples of selected topographies are shown in Figure 2.6.

For the generation of micron-sized surface topographies, picosecond and femtosecond pulses yield similar results, as predicted. By employing fs pulses at sufficiently low fluences (approx. 0.04 J/cm^2), it is possible to generate nanoscale surface roughening. This seems not to be possible with ps pulses, which simply result in generation of micron-sized structures dependent on the laser spot size on the sample. We refer this difference to thermal effects resulting from the picosecond-long pulse, which clears away the small nanometer-sized details, even though the thermal effects are eminently decreased compared to the nanosecond regime.

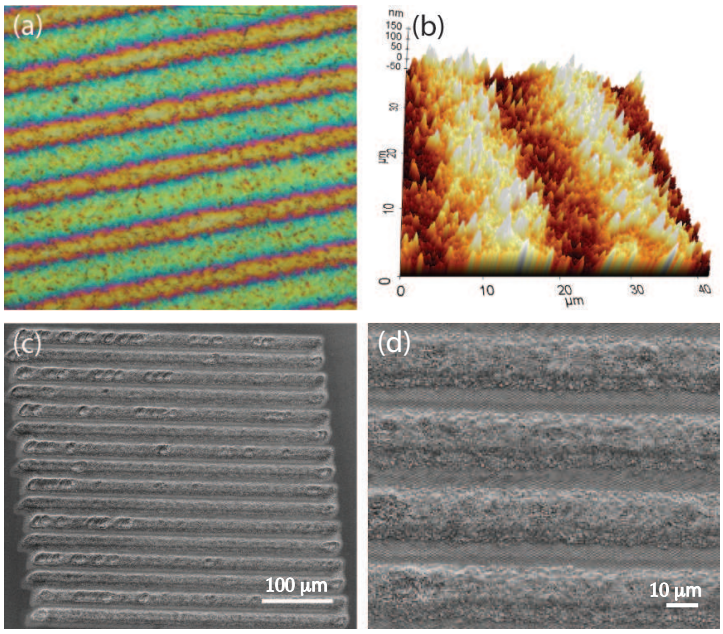

Figure 2.7: Surface topographies created using femtosecond pulses. Optical microscope (a) and AFM (b) images of the nanoscale surface topographies generated at low fluence (0.04 J/cm^2). (c, d) Scanning Electron Microscope images of the micrometer scale surface topographies generated at high fluences (0.89 J/cm^2).

By utilizing femtosecond pulses, we generate nanometer scale surface topographies at low fluences and microscale surface topographies at high fluences. Line textures are generated on the titanium surface with incident power of 1.4 W, repetition rate of 43 MHz, pulse length of 300 femtosecond, scan rate of 4 μm/s, and focal diameter of 10 μm (Figure 2.7(a) and (b)). The corresponding fluence is 0.04 J/cm^2. These parameters result in nanoscale surface modification with a mean roughness of 100 nm.

On the other hand, a similar line texture, however of microscale height, is generated by employing incident power of 0.7 W, repetition rate of 1 MHz (corresponding to a pulse energy of 700 nJ), pulse length of 400 femtosecond, scan rate of 3 μm/s, and focal diameter of 10 μm (Figure 2.7(c) and (d)). The corresponding fluence here is 0.89 J/cm^2. When using fs pulses, there is no heat-affected zone (HAZ) that can be distinguished through scanning electron microscope (SEM) and atomic force microscope (AFM) images. Decreasing heat affected zones is critical since these HAZ are more susceptible to the generation of cracks that decreases the life-time of the biomaterial [55, 56].

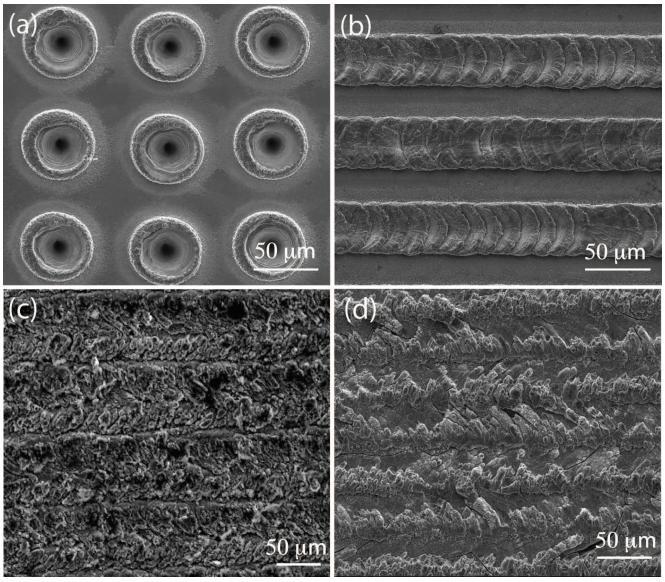

Figure 2.8: SEM images of microscale surface topographies generated with picosecond pulses. Dotted (a) and line-scan (b, c, d) structures.

By using picosecond pulses, microscale surface topographies with 10-20 μm feature sizes and height differences of approx. 5-10 μm are efficiently generated. Figure 2.8(a) shows SEM image of dot-pattern generated on the titanium surface employing incident optical power of 2 W, repetition rate of 43 MHz, pulse duration of 20 picosecond, and approx. 40 μm of focal diameter. The corresponding fluence here is 0.0037 J/cm^2.

A line texture is shown in Figure 2.8(b), generated using incident laser power of 1 W, repetition rate of 1 MHz, pulse length of 80 picosecond, scan rate of 3 μm/sec, and 10 μm of focal diameter. The corresponding fluence is 1.27 J/cm^2. Another texture is shown in Figure 2.8(c), generated using incident laser power of 2 W, 43 MHz repetition rate, pulse length of 25 picosecond, focal diameter of 10 μm, scan rate of 50 μm/sec and fluence of 0.0059 J/cm^2. The texture is generated by line scans, with the parallel scan lines scarcely touching each other at the edges. The line texture in 2.8(d) is generated using the same parameters as in Figure 2.8(c), but the parallel lines are overlapped by more than few micrometers at the edges. In the picosecond regime, a little Heat Affected Zone is distinguishable around the microscale structures, appearing as contrast changes in the SEM images and with an extent of 10-15 μm. The surface textures are mechanically stable and strong. The processed titanium surfaces were repetitively subjected to 10% NaClO in an ultrasonic cleaner and to solutions such as proteolytic enzymes during cell adhesion experiments. Moreover, after almost a year, during which a vast of experiments have been performed, the laser-modified surfaces seem to be unaltered with regard to more recent scanning electron microscope images.

In order to compare the differences between the pulse regimes, we also employ the nanosecond fiber laser to generate surface modifications. A dot-pattern, which is shown in Figure 2.9(a) is created using incident laser power of 1 W, pulse length of 71 nanosecond, repetition of 25 kHz, scan rate of 5 mm/sec, and focal diameter of approx. 40 μm. The corresponding fluence is 3.2 J/cm^2. SEM image of a line texture generated with same laser parameters are demonstrated in Figure 2.9(b). The ns-pulsed laser significantly results in more noticeable Heat Affected Zone, extending up to 50 μm, as well as a relatively decreased repeatability and precision. It seems that for most surface modification applications, the

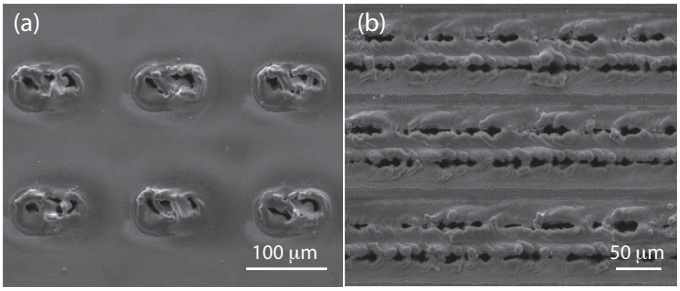

Figure 2.9: SEM images of micrometer-sized surface topographies created with nanosecond pulses. Dotted (a) and line-scan (b) structures.

micrometer scale control afforded by the picosecond fiber laser to be enough. [57].

For a better understanding of the processes behind the formation of the structures, we utilize energy-dispersive X-ray spectroscopy (EDX) analysis and Raman spectroscopy of the modified surfaces. It is possible to generate microstructures, which are pronounced as either protrusions or depressions on the surface. The height differences are around few micrometers and dependent on the laser parameters. The EDX results show that oxygen is present in the modified regions, while it is absent in the non-irradiated fields as shown in Figure 2.10. The concentration of oxygen in surface structures seems to vary in the range of 25% to 35% for any pulse duration. This is consistent with the generation of TiO_2 as a result of the laser modification.

Figure 2.11 depicts the Raman spectra covering 150-750 cm^{-1} of the modified titanium surfaces. As control, the unexposed field of the titanium samples does not show Raman activity. The exposed fields result in three significant peaks located at 241, 439 and 613 cm^{-1}, which can be referred to the multi-photon process, E_g, and A_{1g} active Raman modes for the tetragonal rutile structure of TiO_2, respectively [58, 59]. Thereby, we conclude that the protruding structures generated by laser exposure are mostly composed of TiO_2 in the rutile phase, irrespective of the use of femtosecond, picosecond or nanosecond pulses.

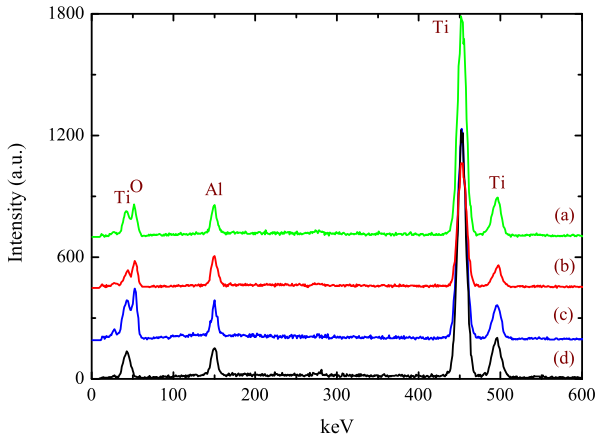

Figure 2.10: EDX analysis of the titanium samples: The irradiated fields are (a) femtosecond, (b) picosecond, (c) nanosecond, and (d) non-irradiated region. The data lines are displaced vertically for clarity.

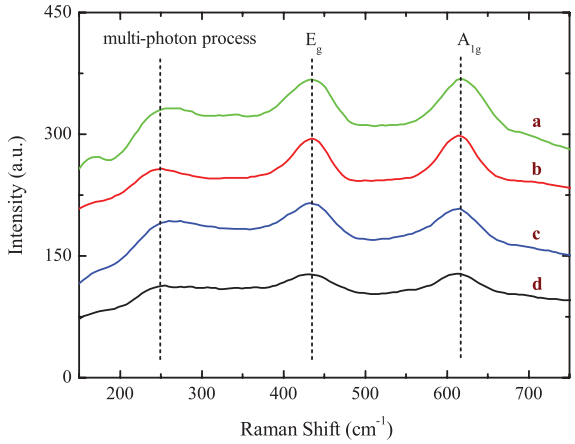

Figure 2.11: Raman spectra of titanium surfaces: The laser-exposed fields by (a) femtosecond, (b) picosecond, (c) nanosecond pulses from the fiber lasers, and (d) non-irradiated field.

2.4.2 Cell Attachment and Proliferation on Laser-Modified Biomaterial Surfaces

The effects of the surface modification on the cell adhesion and proliferation are characterized in vitro via cell culture assays. We compare the picosecond laser-modified surfaces with three different commercially-modified implant surface types modified by acid etching, sand-blasting and the SLA method. Following the methodology explained in the ***Cell Culture*** subsection, we culture cells on surfaces of interest both for 36 hours (Figure 2.12 left panel) to evaluate preliminary surface attachment, and for 7 days to monitor further established cell adhesion and proliferation (Figure 2.12, right panel). Our data demonstrate that ps-pulsed laser modification can be employed efficiently in low-cost laser surface engineering of biomaterials, where distinct fields on the surface can be made cell-adhesion friendly or hostile by using different surface structures.

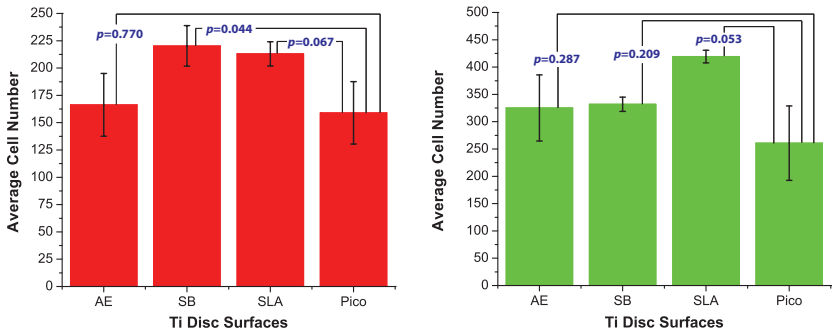

Figure 2.12: Cell counts for analyzing adhesion and proliferation after 36 hours (left) and 7 days (right). p values show the significance of experimental values obtained from commercial surfaces and picosecond laser-modified surfaces according to two tailed t-test. AE: surfaces prepared using acid-etching; SB: surfaces prepared using sandblasting; SLA: surfaces prepared using the SLA technique; Pico: surfaces prepared using the picosecond pulses.

Both cellular adhesion and proliferation responses on picosecond-laser-modified surfaces are as good as commercially-obtained surfaces, which are commonly accepted to be surface modifications of choice for effective tissue integration [60, 61]. Binary comparisons of cellular tests on laser-patterned surface with

other modified surfaces (Acid Etched, Sand-Blasted, or SLA) showed no significant difference with regard to adhesion or proliferation according to a two-tailed t-test, which is confirmed by statistical Bonferroni correction (Figure 2.12). (A p value of <0.02 was considered statistically significant).

Furthermore, we observe a tendency of adhered cells to align along the direction of the linearized structures, which indicates that these laser-generated structures trigger contact guidance response (Figure 2.13(a) and (b)). However, we do not detect significant alignment on the surfaces with nanoscale topographies created with fs pulses (Figure 2.13(c)). Adhesion is not improved either; we referred this to the inadequate interaction between the cells and the nanometer scale surface textures.

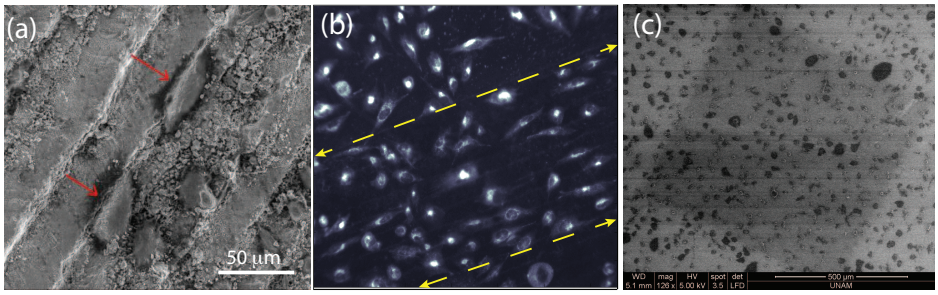

Figure 2.13: (a) SEM image of SaOS-2 cells adhered to a fiber laser-modified titanium sample. The two red arrows indicate the cells aligned with linear structures. (b) Fluorescence microscope image of the same sample. The laser-modified field between the dashed (yellow) lines demonstrates a tendency of the cell population to align along the direction of the arrowheads. (c) SEM image of the cells attached on surfaces with nano-scale topography, which shows no discernible cell alignment.

Moreover, it also seems possible to de-promote cell proliferation and adhesion.With the dotted titanium surface texture, which is shown in Figure 2.14(a), the cells cultured on this surface result in significantly deteriorated proliferation and adhesion. We refer this to the biomechanics of the process: Those holes have diameters approx. 40 μm and depth around 15 μm; cells which drop inside a hole can not adhere and spread properly, hence cannot proliferate. Possibly, they undergo a stress dependent programmed cell death process known as apoptosis,

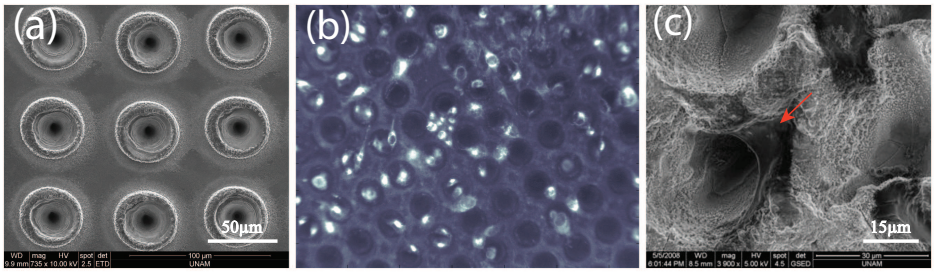

Figure 2.14: (a) SEM image of laser-modified titanium surface with the dotted pattern. (b) Fluorescent image of SaOS-2 cells stained with DAPI and cultured on the dotted pattern. SEM image of same cells on the same pattern; the red arrow indicates a cell at the edge of a hole.

as tested by aberrant nuclear stainings 2.14.

2.5 Conclusion

In conclusion, we demonstrate controlled surface modification of titanium biomedical implant surfaces with in a highly precise and repeatable manner using low-cost picosecond-pulsed and femtosecond-pulsed fiber lasers operating at 1 and 43 MHz repetition rate. To the best of our knowledge, this is the first use of a pulsed fiber laser for surface modification. Additionally, we employ repetition rates approx. 1000 times higher than in previous studies of ultrashort-pulse surface modification. Since the average optical power of the fiber amplifiers and the scanning speed can easily increased, the use of MHz repetition rates offers huge potential for significant advancements in modification speed, subsequently, in the suitability of ultrashort-pulsed surface modification for industrial biomedical applications. Comparison of the surface patterns generated by the picosecond-, femtosecond- and nanosecond-pulsed lasers confirm the predicted trend of reduced thermal effects as the pulse duration is reduced, hence improving repeatability and precision. Nevertheless, we observe that tens of ps-long pulses are sufficient to reliably generate micrometer-scale topographies for control of cell adhesion and

proliferation. Since picosecond mode of the laser does not necessitate a grating compressor, and the laser beam is directly delivered from the optical fiber through a fiber collimator or a fiber focuser, the use of ps pulses at MHz repetition rates offers notable potential for in vivo biomedical studies. Cell adhesion and cell proliferation experiments demonstrate that laser-generated topographies result in performance statistically comparable to commercially modified surfaces that use non-laser-based methods. We find that different surface textures can enhance or inhibit cell proliferation, adhesion and spreading; on the other hand, additional researches are needed for full comprehension of the effect of different textures. An important advantage of laser modification is the ability to selectively process different compartments of a biomaterial surface with different patterns, which may be designed to enhance or inhibit cell responses. Such spatial selectivity is not possible with conventional chemical and mechanical methods.

Although our priority in this thesis study is on modification of titanium-based metal implant surfaces, these results can readily be adapted to different biomaterial types and applications. We believe that ultrashort pulse fiber laser technology is suitable for extensive use in laser surface engineering and related applications outside of the research laboratory.

Chapter 3

Nanosurgery

Thanks to Seydi Yavas for his collaboration in this part of this thesis study.

Ultrashort-pulse lasers are widely used in biological applications in recent years. In addition to their common use in multiphoton imaging and manipulation of single cells at tissue level or even at sub-cellular level, can be achieved using ultrashort pulses with high precision at nanometer-scale. This ability to achieve precise ablation of cellular compartments such as an axon [62] or neuronal spine [63], cellular organelles such as mitochondria [64] or microtubules [65] is known as *nanosurgery*. To date, these researches have employed solid state lasers, especially titanium:sapphire lasers. Although these lasers hold good technical performance, they are very complex to operate, costly and large in size. Their oscillators function only at a repetition rate around 80 MHz and amplified setups are usually constricted to several kHz. In contrast, fiber lasers are simpler to function, more compact and cost much less. More importantly, their pulse repetition rate and pulse train can be adjusted with acousto-optic modulators (AOM). Moreover, their low intensity noise has a high potential in terms of ablation precision. Although fiber lasers have been utilized in two-photon imaging, they have not been employed in nanosurgery to date, despite their apparent high potential. Here in this thesis study, we show for the first time the development of an ultrashort pulse fiber laser-microscope integrated system and its use of for nanosurgery.

3.1 Theoretical Backround of Laser-Tissue Interactions

Basics of laser-tissue interactions is directly interrelated with the physical nature of how light enter into a biological milieu, such as a tissue. The fundamental interaction modes of light with bulk material are reflection, refraction, scattering and absorption as shown in Figure 3.1. The optical behaviour of a material regarding the wavelength of the incoming light, defines the relative contribution of each mode.

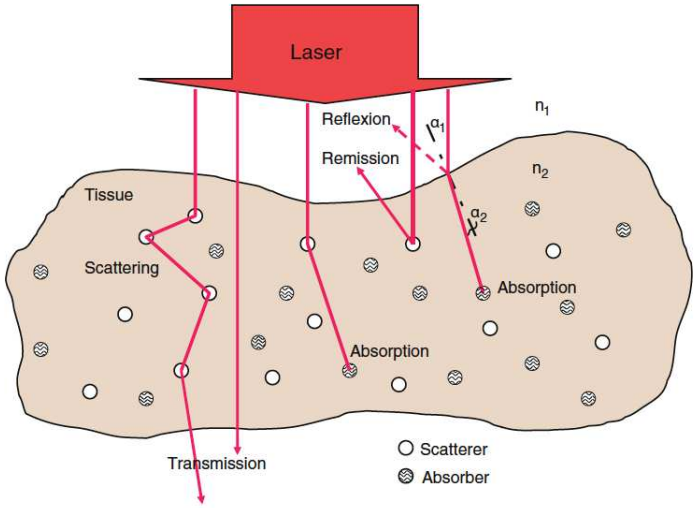

Figure 3.1: Optical interaction modes of a tissue layer with the incident irradiation light. [66]

Reflection means the moving back of light from the surface of a biological tissue without an entry into the tissue. For instance, approximately 4% to 7% of light is reflected off skin [67]. The amount of reflected light increases with higher angle of incidence with the minimum reflection occurring if the laser beam delivered perpendicular to the tissue.

When light hits the surface of the tissue, the portion of the incident light reflects back depending to the angle of incidence, as a result of the refractive

index change. Light penetrating the surface initially is refracted, obeying the Snell's law, which states that the ratio of the sines of the angles of incidence and refraction is equivalent to the reciprocal of the ratio of the indices of refraction:

$$\frac{\sin \alpha_1}{\sin \alpha_2} = \frac{n_2}{n_1} \tag{3.1}$$

In the tissue, light may also be scattered, changing their direction of propagation according to the anisotropy factor, or be absorbed by exciting the absorbing molecule by an electronic transition. Light scattering is present after the light penetrates the tissue. Scattering occurs because of the heterogenous constitution of tissue. Variations in particle sizes and indices of refraction differences between different compartments of the tissue determines the amount of scattering. Scattered light spreads throughout the tissue, which results in irradiation of a larger area of the tissue than anticipated. On the other hand, scattering also limits the depth of penetration due to its occurrence backward as well as forward. In skin for example, a large portion of the light scattering occurs due because of the presence of dermal collagen. Conceptually, the amount of light scattering is inversely proportional to the wavelength of the light. Longer wavelengths scatters in tissue less. On the other hand, as wavelength of the light goes beyond the mid-infrared portion of the electromagnetic spectrum, it will only penetrate superficially, mainly because of the high absorption coefficient of tissue water [68].

The light absorption is primarily responsible for its effects on tissue and this phenomenon is mainly dependent on the constituents of tissue that absorb light and on the wavelength of the incident light. These light-absorbant tissue constituents are known as chromophores. Biological substances such as tissue, have complex structures and chemical compositions, but despite their complexity, their optical features can be generalized by considering the predominant constituents such as water, melanin and hemoglobin [69]. Figure 3.2 depicts the absorption spectra of these three main components. Within the region between 600nm and 1200nm there is a relative decrease in absorption in all three constituents leading to the so-called "near-infrared window in biological tissue or "diagnostic window for light-tissue interactions. Light within that wavelength window penetrates

tissue more efficiently than light in any other wavelength.

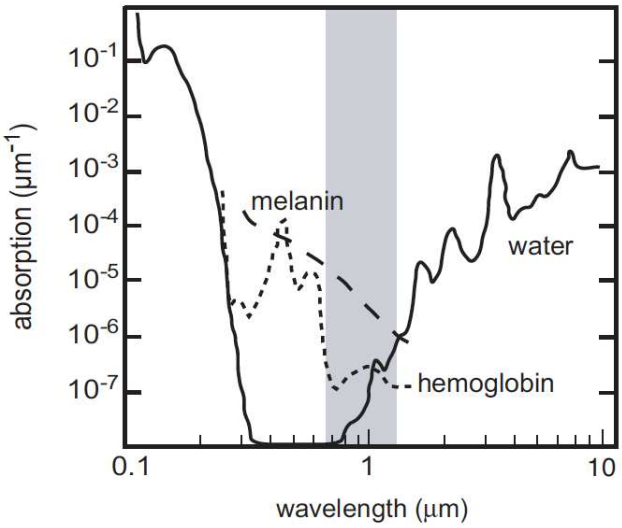

Figure 3.2: Absorption spectra of the major chromophores in tissue and the so-called "near-infrared window in biological tissue. [70]

Characterizing the exact optical features of tissues and the relative contribution of absorption and scattering is a complicated process. Beer-Lambert law relates the attenuation of light to the features of the substance through which light is travelling:

$$T = \frac{I}{I_0} = e^{-\sigma \ell N} \tag{3.2}$$

The law points that there is a logarithmic relation between the transmission of light through a material (T), the attenuation crossection (σ), the distance the light travels through the material (ℓ) and the concentration of attenuating medium (N). I_0 and I are the power intensity of the incident radiation and the transmitted radiation, respectively. σ is the attenuation crossection, which is a product of combination of the scattering and absorption coefficients.

On the other hand, a biological tissue can be highly inhomogeneous and there can be a significant variation from one tissue to another. For instance a corneal

tissue can differ tremendously from a skin tissue, thereby, the penetration depth might vary in orders of magnitude between different types of tissues. Understanding optical features of the biological sample is crucial for determining the optimal laser parameters for a desired application. Variations in laser energy, wavelength and pulse duration can lead to drastically different results, therefore these factors need to be adjusted accordingly for a specific type of application.

In addition to this, a basic understanding of how lasers work and interact with tissue will enable the biomedical researcher or the medical doctor to choose the most suitable laser for a particular biomedical/clinical situation. Even though the physical laws directing laser design are quite complex, the basic principles can be summarized as they are befitting to a biologist or physician.

Laser light has a few unique properties that makes it different from other light sources. Its features such as coherence, monochromicitym, high power and collimation are the key parameters for the clinical applications of lasers. Basically, non-laser light sources emit light of many wavelengths modulated by a cut-off filter. In contrast, laser light is monochromatic, which means that the light emitted by a laser is of almost a single, discrete wavelength determined by the lasing medium. Monochromaticity of lasers is one of the most critical properties for the application of laser-based tools in biomedical or clinical practices because different tissues with different chromophores has different absorption spectra. Thereby, the particular wavelength of laser light influences its penetration depth into tissue. Principally penetration depth of laser light increases as the wavelength becomes higher within the spectrum of visible light, therefore, the particular wavelength absorbed by the tissue should be considered when a laser is utilized for clinical or biomedical use.

Another important characteristic of lasers is that they are collimated. Collimation basically indicates the parallel nature of the emitted laser waves. Because the waves of laser light propagate collimated, the tendency toward divergence is low. By means of this coordinated pattern of light, a laser beam can propagate across long distances with very small loss of light by spreading.

High powers or energy levels that lasers can reach is one of the most important

features of lasers. The amplification process within the laser cavity generates a high density of power. Power and energy both quantify the laser emitted light amount. Energy, which is measured in joules, refers to work and power is the ratio of doing work. It is equivalent to an amount of energy consumed (joules per second). Fluence means the density of energy of a laser beam is measured in joules per square centimeter. Irradiance, which is the density of power of a laser beam, refers to the laser power divided by the area of the incident laser beam which is spot size, and is measured as watts per square centimeter. By manipulating and adjusting each of these parameters, one can tailor the use of laser for specific clinical uses [71].

Consequently. laser radiation can be defined as a concentrated spatial and spectral beam of light. In parallel to this, it is also possible to qualify the beam as a temporal concentration by considering that the emitted photons are condensed into short energetic pulses.

Optical pulses are momentary flashes of light, which are often produced by lasers (pulsed lasers) and delivered in the form of laser beams. Dependent on the hugely high optical frequencies, laser pulses can be drastically short, ultrashort, if their optical bandwidth covers a significant portion of the average frequency. Depending on the short pulse lengths and the potential for tight focusing, laser pulses can be utilized for reaching extraordinarily high optical intensities even with moderate pulse energies. For instance, a 10 femtosecond pulse having only 10 mJ energy has a peak power of the order of 1 terawatts (1000 gigawatts), corresponding to the joined power of approx. 1000 large nuclear power plants. And that optical power can be focused to an area of only a couple of micrometers in diameter. Optical pulses generated can be extremely short, although there is no widespread acception of the definition of "ultrashort", this epithet usually refers to pulses with durations shorter than a couple of tens of picoseconds, and often with the durations of femtoseconds. It should be noted that ultrashort pulse lasers are also called as "ultrafast lasers, but actually they are not faster, which means that they do not have a higher velocity than longer pulses. However, they make it possible to probe and manipulate the ultrafast processes and to transmit optical data faster.

Taken all together, short and ultrashort pulse laser light focused through a microscope objective with a high numerical aperture (NA) can be utilized to achieve highly precise and localized effects inside biological media, which are transparent at low irradiance [72]. Quantitative estimations of the energy transport in laser irradiated transparent materials, such as cells, indicates that laser radiation mainly interacts with the electronic system.The deposited energy is then transferred to the lattice as heat via collisions with phonons. For very short pulses both processes can be temporarily decoupled. For pulses longer than a few tens of picoseconds, the generally accepted context of laser damage/ablation is based on the heating of conduction band electrons by the incident radiation and transfer of this energy to the lattice in a quasi-equilibrium, steady-state fashion during the laser pulse (in a photon-electron-phonon and electron-phonon interaction). Damage occurs via conventional heat deposition resulting in a phase transformation of the dielectric material [73]. In order to reach the breakdown level, the transparent, dielectric material is initially transformed into an absorber, so a high density of electrons are "pumped into the conduction band, so that the process of plasma generation via laser-induced breakdown in transparent biological milieu occurs. It substantially comprises the generation of quasi-free electrons by both with photoionization and avalanche ionization and it has been experimentally demonstrated that the threshold of the optical breakdown in water, in ocular and in other biological milieu are significantly comparable [74]. Hence, describing the breakdown process in water can be a model for the processes in biological media.

To explain the breakdown process in water, it is proposed that water must be assumed as an amorphous semiconductor and its excitation energy, which is the energy needed for a transition from the molecular 1b1 orbital into an excitation band, which is band gap, is calculated as 6.5 eV [75, 76]. Given that the photon energies at the wavelengths of 1064nm, 800 nm, 532 nm, and 355 nm are 1.17 eV, 1.56 eV, 2.34 eV, and 3.51 eV, respectively, the energy of six, five, three, and two photons, respectively, is necessary to exceed the band gap energy of 6.5 eV. This excitation energy into the conduction band for water, can be provided either by photoionization (multiphoton ionization or tunneling or by impact ionization [73, 74].

Multiphoton and tunneling ionization are the fundamental mechanisms that direct photoionization at different frequencies and field strengths of the electromagnetic field. Keldysh introduced a factor $\gamma = \omega/\omega_t$ to distinguish tunneling and multiphoton ionization regimes, where $1/\omega_t$ refers to the time for tunneling through the atomic potential barrier, which is inversely proportional to the electromagnetic field strength [77]. For values that $\gamma \ll 1$ as obtained with lower frequencies and large field strengths, tunneling is mainly responsible for ionization, while for values $\gamma \gg 1$ the probability of multiphoton ionization is much higher than that of tunneling ionization. Femtosecond optical breakdown necessitates much higher field strengths. For $\lambda = 800$ nm, the transition from multiphoton to tunneling ionization occurs at field strengths of about 100-200 MV/cm, corresponding to laser irradiances of 1.3-2.6 x 10^{13} W/cm^2 [73], thus, values for the breakdown irradiance for a 100 femtosecond pulse in demonised water, which is around 1.1 x 10^{13} W/cm^2 for $\lambda = 580$ nm) are close to this transition [74].

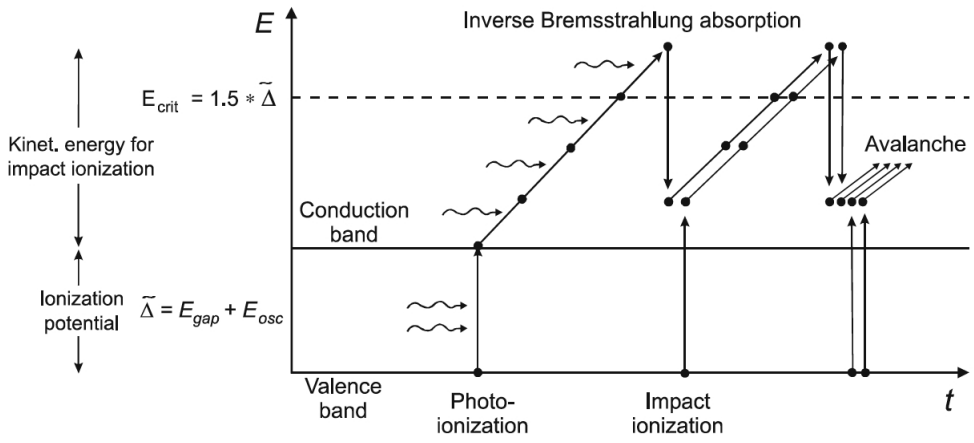

Figure 3.3: Photoionization, inverse Bremsstrahlung absorption, and impact ionization during the process of plasma formation. Repeated sequences of inverse Bremsstrahlung events and impact ionization trigger an avalanche growth in the amount of free electrons. [74]

Once a free electron is created in the milieu, through such ionization modes, it can absorb photons in a non-resonant process called "inverse Bremsstrahlung"

(Figure 3.3). This electron gains kinetic energy during the absorption of the photon. After a chain of several absorptions, the kinetic energy becomes sufficient to produce another free electron through impact ionization. Two free electrons with low kinetic energies are now available, which can acquire energy via inverse Bremsstrahlung absorption.The repetitive chain of inverse Bremsstrahlung absorption events and impact ionization leads to an avalanche increase in the number of free electrons when the irradiance is sufficiently high to overcome the free electron losses due to the diffusion out of the focal volume. Consequently, a low-density plasma occurs.

Considering that the plasma occurs in water, the creation of radical oxygen species such as H_2O_2 and OH^- through various pathways following ionization and dissociation of water molecules, primarily causes cell damage. Capture of electrons into an antibonding molecular orbital may trigger fractionation of biomolecules, e.g., for a molecule XY, such process refers to:

$e^- + \mathrm{XY} \rightarrow \mathrm{XY}\bullet\text{-}$

where the XY•- has a repulsive potential along the X-Y bond. After a time about 10^{-15} to 10^{-11} seconds (from femto- to picoseconds), the transient molecular anion state decays by

$\mathrm{XY}\bullet\text{-} \rightarrow \mathrm{X}\bullet + \mathrm{Y}\text{-}$

These radical species are extremely reactive and known to cause cell damage [78]. Such chemical reactions during the breakdown event have little practical relevance for large radiant exposures producing a high density of plasma energy, because in such conditions the tissue effects are dominated by major thermomechanical effects. Nevertheless, these chemical reactions are of great importance for femtosecond plasmas, which leads to tightly-localized chemically-mediated ablation or dissection events.

Such uses of pulse lasers began in the 1980s with intraocular surgery by using nanosecond pulse lasers [79]. After the development of femtosecond lasers, corneal refractive surgery was also performed, via femtosecond lasers [80]. As the

laser pulse duration becomes shorter, the nonlinear propagation effects become more important and a larger laser power densities are required to produce optical breakdown. Thus, it is not possible to have tightly localized energy deposition when ultrashort pulses are focused into the bulk of transparent milieu (such as cells) at low NA. As described above, for optical breakdown to occur, an irradiance threshold to be exceeded. As the NA increases, the spot size decreases and thus the power density that is required to overcome the irradiance threshold decreases. For femtosecond optical breakdown in water and glass this was found to be the case for NA $\geq$ 0.9 [81].

3.2 Cellular Applications of Ultrashort-pulsed Laser Nanosurgery

Ultrafast lasers are employed in diverse range of biological applications, particularly in the last decade. In addition to their routine use in two-photon imaging [82], individual cell modification and ablation of intracellular structures can also be achieved by using ultrashort pulses with high precision [83]. The precise ablation of sub-cellular structures such as microtubules [84], or cellular organelles such as mitochondria [85] is commonly known as *nanosurgery*. In parallel, similar experimental methodology is increasingly used in other fields of cellular biology. A novel approach is using ultrafast lasers for delivering exogenous materials such as DNA or RNA, into cells [86], such that, when this method is compared to the more common techniques of biotechnology such as cationic polymer based transfection, efficiency of laserfection is significantly higher. Taken all together, proof-of-concept studies demonstrate that ultrashort-pulsed laser nanosurgery is a promising technique in cell biology and yet this technique appear to have begun to be employed as a laboratory tool by cell biologists, already. A diverse range of studies show that nanosurgery represents an innovative and useful method for both in vitro and in vivo researches.

The first study that performed sub-cellular nanosurgery was dissection of chromosomes with nanometer precision [87]. Since then, various other nanosurgical operations rapidly followed. As the number of publications indicating that nanosurgery can be used as a research tool accumulated over the time, researchers have begun taking advantage of this technique for basic cell biology studies. An example is the ablation of the centrosome organelle in mouse hippocampal neurons [88]. In this publication, it was demonstrated that after the ablation of centrosomes, axons regenerated through an acentrosomal microtubule nucleation point and continued to grow.

In another recent study, an ongoing debate on the synthesis of Golgi apparatus in mammalian cells, which is either Golgi is synthesised de novo or not, was tested. Ultrashort pulse lasers were utilized in order to elucidate this biological controversy on Golgi complex [89]. In this study, the data presented within this work provide evidence supporting the de novo Golgi synthesis hypothesis in mammalian cells.

Ultrafast laser nanosurgery was also utilized in a recent botanical research [90]. Researchers constructed their experimental design based on the phenomenon that neighboring epidermal cells on guard cells push these guard cells and resulting in movement of stoma; thus they performed the ablation experiment such that a microhole on the surface of epidermal cells caused shrinkage of these epidermal cells and this triggered opening of nearest stoma. They showed that immediately after the laser-induced stomatal opening, ERs localization changed due to the mechanical stress caused by stoma opening.

On the other hand, majority of the earliest results utilizing ultrafast laser nanosurgery came from cytoskeletal photodisruption studies. In 2005, researchers cut the phalloidin-labelled actin fibers of fixated NIH/3T3 fibroblast cells as shown in Figure 3.4 [91]. Based on the applied pulse energies, researchers examined the differences between the photobleach effect and actual material removal. It was claimed that at pulse energies of 1.5 nJ, material ablation is still observed, however, at 1 nJ, photobleaching dominates and thereby it was suggested that there is a pulse energy threshold at 1.5 nJ for 100 femtosecond laser pulses at 800

nm focused with a 1.4-NA objective, in order to make actual cuts on chemically fixated cells.

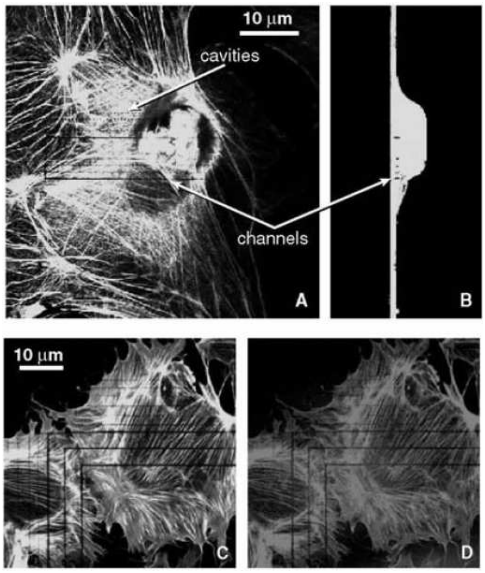

Figure 3.4: Laser confocal microscopic images of a fixated 3T3 fibroblast stained for F-actin with a green fluorescent dye. (A) Top view of a mid-plane horizontal section through the cell showing channels and cavities produced by femtosecond laser ablation. The top and bottom channel were obtained at a pulse energy of 3 nJ; those in between at pulse energies ranging from 1.5 to 2.3 nJ. (B) Reconstructed orthogonal image of the same cell. (C) A cell that was prestained for F-actin with a green fluorescent dye immediately after ablation with 2-nJ (widechannels) and 1.5-nJ (narrow channels) laser pulses. (D) The same irradiated cell after restaining for F-actin with a red fluorescent dye. [91]

In addition to the nanosurgery applications on cytosolic compartments, nuclear elements were also specifically ablated via optical pulses. A recent example is the demonstration of a telomere-associated protein (TRF2) having an important function in DNA damage response [92]. A femtosecond laser is employed to generate double-strand breaks (DSBs) at specific locations of DNA inside the nucleus, and the presented data showed that endogenous TRF2, a telomere associated protein, accumulated at laser induced DSB sites.

In another study demonstrating the use of laser nanosurgery on cell nucleus,

the human chromosome 1 was dissected with a full width half maximum (FWHM) cut size of 100 nanometers, in which the ablated area corresponding to the 1/400 of the chromosome and to ∼65kb chromosomal DNA [93] (Figure 3.5). Even smaller cut sizes below 50 nanometers have been achieved by exploiting metal nanoparticles as laser light antennas [94].

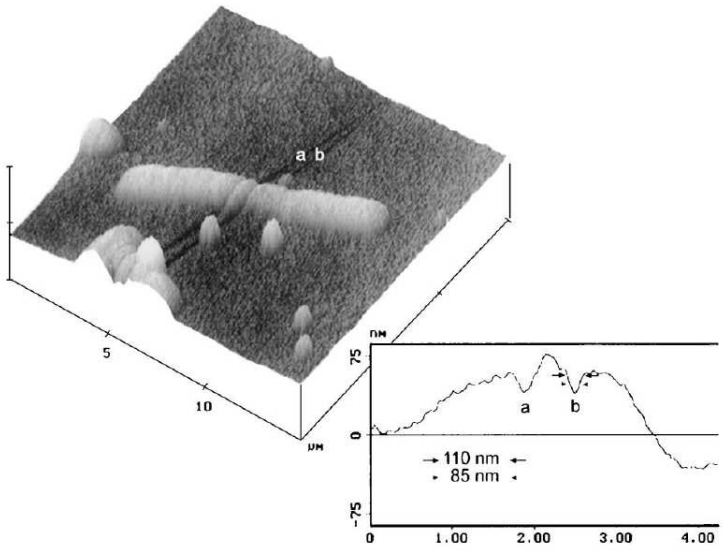

Figure 3.5: Topographical image and depth profile of two laser cuts on chromosome 1. Material was partially removed, as indicated in the depth profile. A sub-100-nm FWHM cut size was determined. [93]

As shown, ultrashort-pulsed nanosurgery technique allowed researchers to directly manipulate such an important cellular compartment and offered a novel capacity for in situ investigation of nuclear structure

Delivery of nucleic acids such as a plasmid DNA or siRNA inside cells is termed as transfection, which is originally a molecular technique routinely used by cell biologists. Most of the common transfection methods such as cationic polymers, liposomes or electroporation are used to deliver nucleic acids to large populations of living cells arbitrarily. Although these methods work efciently on many cell lines, there are some certain cell types such as embryonic stem cells, primary cell cultures and neuronal cells that are difficult to transfect via these

common methods. Optical transfection, or laserfection, is a recent method that has been demonstrated to have worked efficiently on these difficult-to-transfect cells. In a recent study, researchers utilized laserfection in order to deliver the Channelrhodopsin2-YFP plasmid construct into primary retinal ganglion neurons from goldfish [95]. Hence, optoinjection or optical injection is a technique that al-lows exogenous delivery of various membrane impermeable substances into a cell using light. Although use of lasers for optical material transfer into the cells dates back to 1980s [96], ultrafast laser based delivery method is relatively new and likely to be more efficient and permit higher survival capacity.

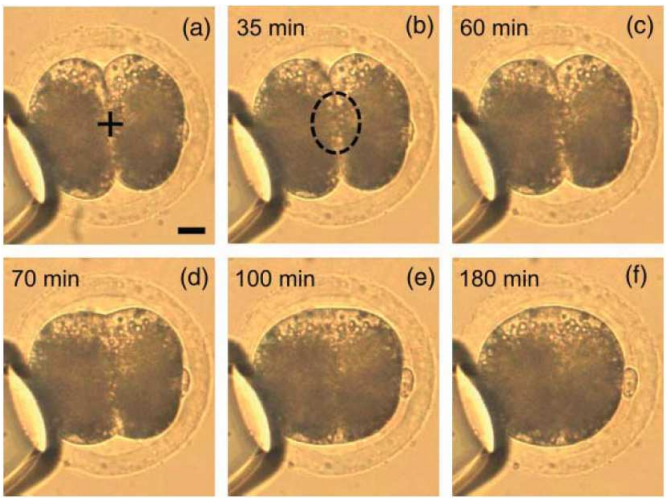

Figure 3.6: Femtosecond laser-induced fusion of two-cell porcine embryo. (a) Irradiation of the cell-cell junction (indicated by black cross) triggered cell fusion. (b) Cytoplasmic streaming between both cells occurred about half an hour after laser treatment (indicated by dashed ellipse). (c) and (e) Cell fusion proceeds. Scale bar: 20 μm. [97]

Cell fusion is a natural phenomenon that has roles in various biological events such as fertilization, formation of muscle fibers and generation of certain types of bone cells [36]. In addition to this, it is believed that this phenomenon takes place in carcinogenesis as well [98]. Biologists have intensively studied on this phenomenon and developed various bioengineering techniques based on viruses, chemical reagents or electrical discharge, in order to achieve artificial cell fusion. Although laser induced cell fusion method dates back to 1990s [99], ultrafast

laser-induced fusion of cells has recently been demonstrated, on two sister cells within a parthenogenetic porcine embryo as shown in Figure 3.6 [97]. Long-term assessment of vitality indicated that incubated fused cell survived more than 6 days in culture conditions specific for porcine embryo development.

Biophotonic methods such as caging/uncaging, optogenetics and super-resolution microscopy have had a great deal of contribution to neurobiology researches, so that there is clearly an emerging subfield as neurobiophotonics. In addition to their well-known use in nonlinear microscopy, ultrafast lasers are being used for direct manipulation of neurons especially for the last ten years. An example is direct nonlinear stimulation of neurons via ultrashort pulses, as a multiphoton version of the Fork experiment performed in 1971 [100]. In a recent example, researchers utilizied ultrashort laser pulses to directly stimulate excitable neurons in order to identify the functional topology of a neuronal circuit and measured the calcium responses with a calcium-sensitive dye [101] (Figure 3.7).

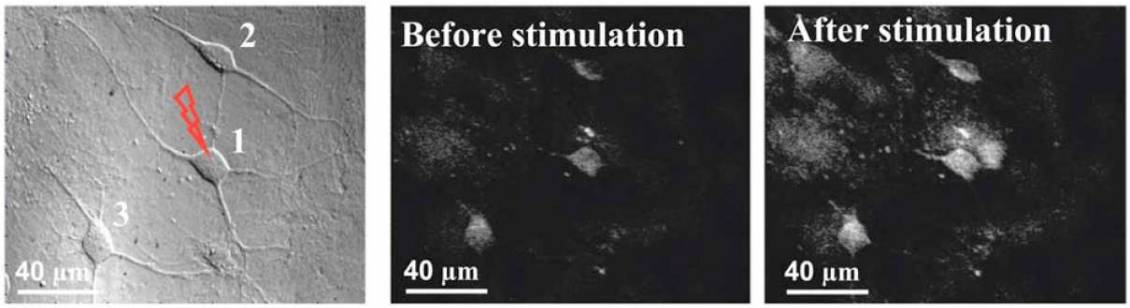

Figure 3.7: Responses of neurons to the pulsed-laser stimulation. DIC image and fluorescence images of a Fluo-4-labeled neural circuit before and after stimulation. The lightning symbol indicates that N1 was irradiated with the femtosecond laser. [101]

Ultrashort-pulsed laser nanosurgery is a novel research field and offers a broad range of application. Over the past decade, plenty of proof-of-principle study demonstrated that this method is highly efficient and provides superior control

both on spatial and temporal resolution. In addition to all these advancements in ultrashort-pulsed biophotonics, fiber laser systems offer a high compatibility for being used outside the research laboratory, which is a substantial necessity for industrial and biomedical applications. Furthermore, ultrafast fiber lasers, with their apparent advantages such as long-term stability in operation, have a high potential in a wide range of scientific and biomedical applications.

Hence, in this part of this thesis study, we develop a custom-built ultrafast fiber laser-based microscope system for nanosurgery and tissue ablation experiments. Furthermore, we applied this system for doing high-precision dissections, to a diverse range of biological specimens ranging from the tissue level to subcellular level, such as a part of a neuron or a single mitochondrion. Finally, we upgraded this integrated system such that, through the use of Acusto Optical Modulaters and custom-developed Fieled Programmable Gate Arrays, it can create arbitrary pulse patterns without limitations.

3.3 Experimental Methods

3.3.1 Imaging

3.3.1.1 Microscopy

For real-time imaging of the biological sample, a customized epi-fluorescent microscope (Nikon Eclipse Ti-U) is used. The laser beam is directed to the objective with a dichroic mirror housed in an extra turret. The dichroic mirror is highly reflective at the laser wavelength, while transmitting visible light and fluorescence excitation. Sample positioning is accomplished via a step-motor based 2-D micropositioning stage (with a precision of $\sim$1 μm) and a 3-D piezo stage with $\sim$20 nm precision. For most applications, the micropositioning stage alone provides sufficient resolution. Visualization is based on both fluorescent and phase-contrast imaging. A 60X,1.2-NA objective and a 100X, 1.3-NA objective are used

interchangeably for sub-cellular ablation and a 20X, 0.4-NA, phase-contrast objective is used for multicellular/tissue-level ablation, on both cases, together with a high-sensitivity EMCCD camera is used for imaging. All major aspects of the laser-microscope system, including control of the FPGA system for pulse picking and gating, positioning of the sample, control of the camera and image acquisition are controlled via a computer for nearly completely hands-free operation. An analog computer joystick allows ease of use for positioning.

3.3.1.2 Fixation and Staining

For the ablation experiments performed on fixated cells, attached cells are washed with PBS and then fixated in 0.1 M sodium cacodylate buffer with 3% glutaraldehyde, pH 7.2 at 4°C overnight, the day before the ablation experiments. For mitochondrial ablation experiments, following up the fixation stage, cells are stained with 300 nM 4, 6-diamidino-2-phenylindole, dilactate (DAPI, dilactate) in PBS and with 250 nM Mitotracker Red 580 (Invitrogen) in the corresponding cell culture medium.

3.3.2 Cell Culture

3.3.2.1 Cell lines and Growth conditions

Human osteosarcoma cell line SaOS-2 and rat pheochromacytoma cell line PC12 are used for nanosurgery experiments. SaOS-2 cells are cultured in McCoys 5A medium supplemented with 15% fetal bovine serum, 2 mM L-glutamine, streptomycin/penicillin 100 U/mL, and in a humidified atmosphere of 95% air and 5% CO_2 at 37°C. For PC12 cells, two different cell culture media are used: Growth medium and differentiation medium. Growth medium consists of RPMI 1640 supplemented with 10% heat inactivated horse serum (HIHS), 5% fetal bovine serum, 2 mM L-glutamine and 100 U/mL streptomycin/penicillin; this medium is used for routine subculturing of undifferentiated PC12 cells. Differentiation medium has the same ingredients, but does not contain FBS, has a reduced amount of

HIHS as 1% and contains 100 ng/mL nerve growth factor (NGF). Both cell lines are incubated in a humidified atmosphere of 95% air and 5% CO_2 at 37°C. For all experiments, cells in 1 mL of medium were plated onto 35 mm coverglass-bottom culture dishes (Bioptechs). For PC12 cells, dishes are previously coated with Collagen A (PAN Biotech) according to the manufacturer-recommended procedure. Growth media are exchanged three times weekly.

3.3.2.2 Cryopreservation of Stock Cells

For both of the cell lines, same procedure applied: Exponentially growing cells in 100mm cell culture plate were harvested by trypsinization in the case of SaOS-2 and by force-pipetting in the case of PC12, and then collected in 5 ml growth medium. Then, cells were precipitated at 1500 rpm for 3 min. The pellet was suspended in a freezing medium (8% DMSO, 92% FBS). Pellets were resuspended in 1ml freezing medium in cryotubes and they were left at -20°C overnight. The next day cells were stored at -80°C for 1 day to 1 month. Finally, the tubes were transferred into the liquid nitrogen storage tank for future experiments.

3.3.2.3 Thawing of Frozen Cells

For both of the cell lines, same procedure applied: The frozen cell line was taken from the liquid nitrogen tank and immediately put on ice and then placed into a 37°C water bath for 1-2 minutes. The cells were transferred into 15ml tubes and resuspended in 9ml growth medium. The cells were centrifuged at 1500 rpm for 3 minutes. Supernatant was discarded and the pellet was resuspended in 10 ml culture medium to be plated into 100 mm dish. After overnight incubation culture mediums were replenished.

3.4 Results

The experimental setup, which includes the microscope, custom-built electronics and the fiber laser is depicted schematically in Figure 3.8.

The seed oscillator is an Yb-doped fiber laser, functioning in the all-normal-dispersion regime [51]. The choice of this mode-locked regime is because of the fact that it is an extremely robust system, such that this mode-locking regime generates relatively longer and structured pulses. On the other hand, the amplifier part efficiently determines the pulse duration, which is a result of gain narrowing and residual higher-order dispersion [102]. The oscillator comprises a 5 m-long section of single-mode fiber (SMF, of the type HI-1060) and 0.6 m-long Yb-doped fiber, followed by another 0.4 m of SMF. Net group velocity dispersion, GVD_{net}, of the oscillator is calculated to be around 0.138 ps^2. The gain fiber is pumped in core with a pump diode delivering 310 mW of power through a 980/1030 nm wavelength division multiplexer. Unidirectional operation is ensured using an in-line optical isolator. Mode-locking is initiated and stabilized by nonlinear polarization evolution. Single pulse operation of the laser output is verified via long-range autocorrelation against bound pulse generation and RF spectral measurements (with up to 12 GHz) against regular multiple pulsing. The in-line amplifier system consists of a fiber stretcher, a fiber-pigtailed Acusto-Optical Modulator, and three gain stages.

The first two stages are core-pumped. The final stage is cladding-pumped, where pump light is delivered through a signal-pump combiner. The lengths of single-mode Yb-doped fibers used for pre-amplifier and amplifier stages are 1 m and 0.5 m, respectively. The core diameters are 6 μm. First stage is pumped with 300 mW pump power in the forward direction and the second stage is pumped with 120 mW in the backward direction. The final stage consists of a 2 m-long Yb-doped fiber with 20 μm core, 125 μm cladding diameters and numerical aperture of 0.08. The gain fiber is pumped in the forward direction with a pump diode laser producing 2 W centered around 976 nm. The beam extracted from the amplifier using a fiber-coupled collimator. The amplified pulses are dechirped in a standard diffraction grating compressor.

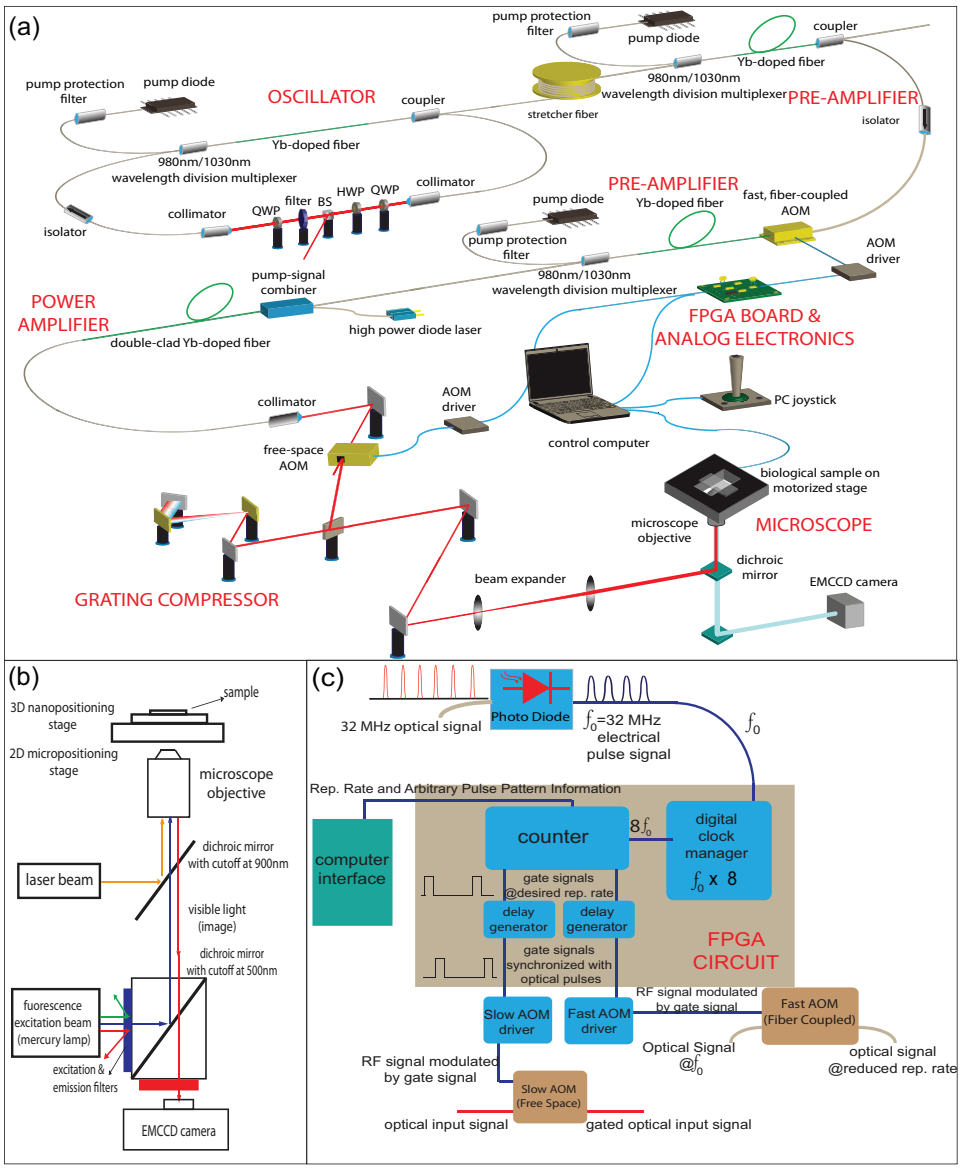

Figure 3.8: (a) Schematic of the experimental setup. FPGA: field programmable gate array; AOM: acousto-optic modulator. (b) Schematic of the laser-fluorescence microscope optics. (c) Schematic of the FPGA and analog electronic circuitry.

The oscillator mode-locks readily and maintains its modelock with a characteristic optical spectrum depicted in Figure 3.9(a).

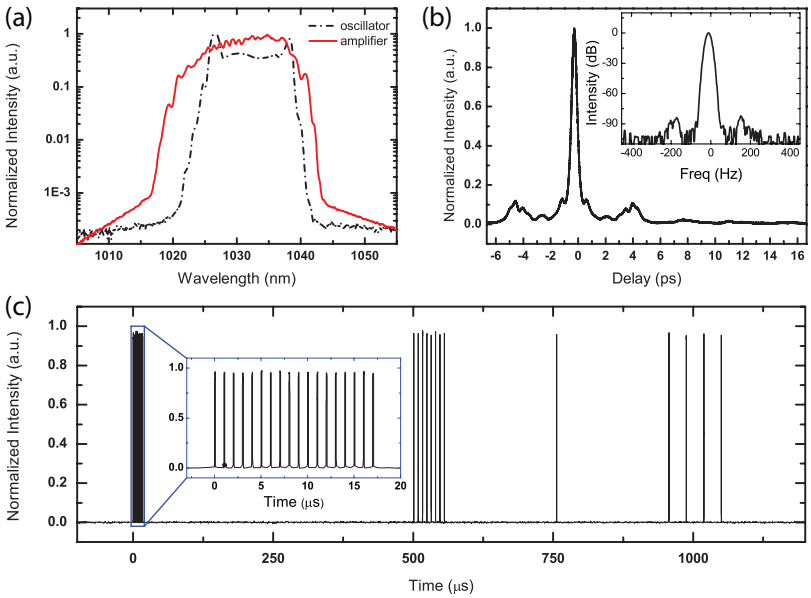

Figure 3.9: ((a) Optical spectrum of the oscillator and amplifier outputs. (b) Autocorrelation of the amplified pulses after dechirping. Inset: Close-in RF spectrum around the repetition frequency. (c) Measured pulse train, exhibiting a complex pulse sequence as an example. Apparent variations in the pulse heights due to digital sampling are not real.

The oscillator generates 3-ps-long chirped pulses with a bandwidth of 15 nm at a repetition rate of 32.7 MHz. Output coupling from the cavity is achieved through a %20 output coupler, which delivers 32 mW of average power to the fiber stretcher, which consists of 40 m of single mode fiber (HI-1060). Pulses are stretched to ∼35 ps and then amplified to 4.5 nJ energy per pulse in the first amplifier stage. After the first amplifier stage, repetition rate of the pulses are decreased to a desired repetition rate, which can be selected between 1.02 to 32.7 MHz, depending on the application. The role of the second amplifier stage is to recompense the decrease in power due to pulse picking in the AOM (the insertion loss is ∼4 dB, in addition to losses due to pulse elimination), producing approximately 110 mW of average power, virtually independent of the pulse picking frequency in the AOM. The final power amplifier operates as a power booster to

reach pulse energies required for ablation of the biological specimens, with a maximum pulse energy of ∼125 nJ, which corresponds to an average optical power of 500 mW at 4.08 MHz repetition rate. The laser system itself is not limited in terms of optical average power (with a similar configuration, we were able to reach 50 W), but somehow limited in terms of pulse energy due to nonlinear effects. Nevertheless, the damage threshold of the microscope objectives indirectly limits the average power. After dechirping in the grating compressor, the compressed pulse duration is around 240 fs. The optical spectrum of the chirped, amplified pulses and autocorrelation after dechirping are shown in Figure 3.9. A second, free-space AOM is integrated into the system for gating of the individual pulses, which allows the exact control of the exposure time of the irradiation on the specimen as well as the further reduction of the repetition rate down to 1 kHz or formation of pulse bursts (Figure 3.9(c)).

The pulse picking is handled by home-built FPGA to pick pulses at two acousto-optic modulators located after the amplifier stages. The FPGA is controlled with a user interface software operating on a personal computer. A fraction of the laser optical signal is detected at a fast photodiode and the output is fed to the FPGA as the clock source. In order to obtain a better temporal resolution in picking out the optical pulses, a faster clock signal is needed. Thus, the clock signal derived from the repetition rate of the laser, is multiplied by 8 at the digital clock manager inside the FPGA to ∼262 MHz. A one-time-only delay adjustment in the FPGA allows the new clock signal to be fully synchronized to arriving optical pulses at the AOMs. The FPGA starts counting the pulses and sends gating signal to the AOM drivers when a pulse is to be picked. As well as picking out the pulses continuously, the system is able to work in arbitrary picking mode. Thereby, the end-user is enabled to pick and drop any number of pulses through the software interface, which can be adjusted to generate a desired pulse sequence upon the press of a button. There are virtually no limitations on the pulse sequences that can be generated. All major constituents of the laser-microscope setup, including control of the FPGA part for pulse picking and gating, sample positoning, image acquisition and camera control are controlled through a computer for almost completely hands-free functioning.

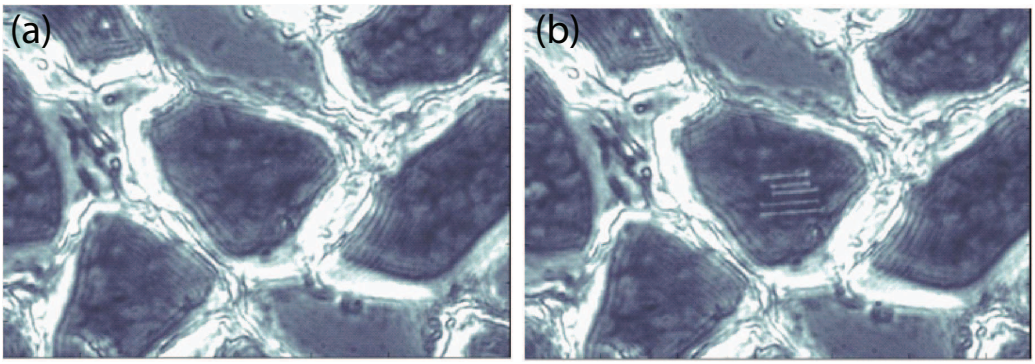

Figure 3.10: Mouse gastrocnemius muscle tissue slice (a) before and (b) after laser surgery (5 parallel cuts are clearly visible); 4.08 MHz, 240-fs, 7-nJ.

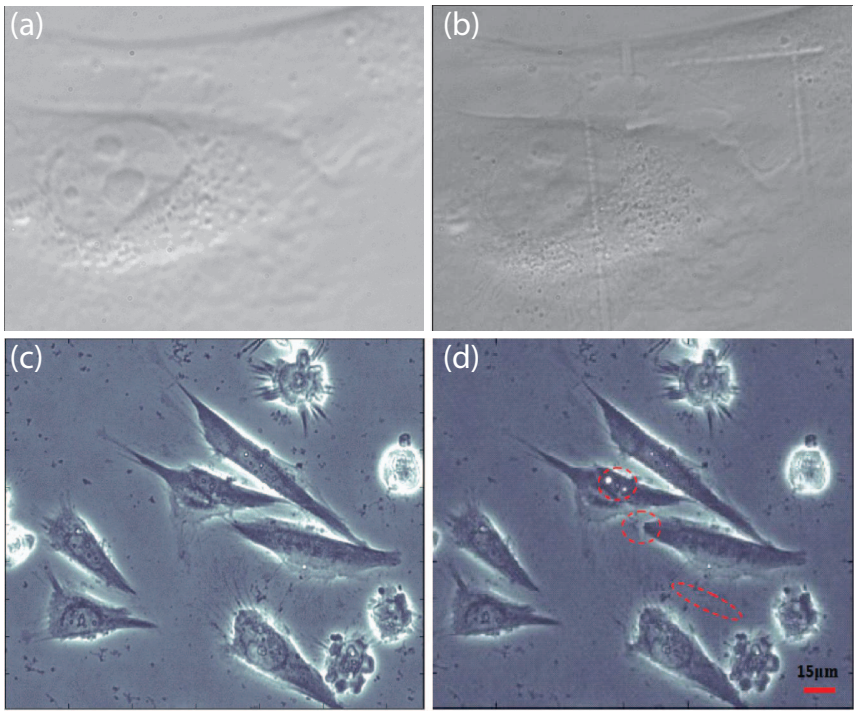

Figure 3.11: Fixated SaOS-2 cells (a) and (c) before; (b) and (d) after femtosecond nanosurgery; 4.08 MHz, 240-fs, 7 nJ.

First, in order to test the system's effectiveness on laser surgery of biological samples; 240 femtosecond, 7-nJ pulses at 4.08 MHz are used to create cuts on frozen sections of mouse gastrocnemius muscle. With the 20X objective, the laser beam is focused to a spot size of ~ 2.2 μm. With the optical telescope at the back port of the microscope, the back apertures of the 60X and 100X objectives are completely filled, this results in underfilling of the 20X objective. On the tissue section, 5 parallel and linear cuts are created, as shown in Figure 3.10. The widths of the lines are measured to be $2 - 2.5$ μm, which is consistent with the incident spot size.

Then, femtosecond nanosurgery is applied on chemically fixated SaOS-2 cells utilizing the 100X objective; linear cuts are clearly visible in Figure 3.11(b). Femtosecond photodisruption is replicated by using 60X objective and repeated on chemically fixated SaOS-2 cells. In this experiment, sub-micron features are observed as shown in Figure 3.11(d).

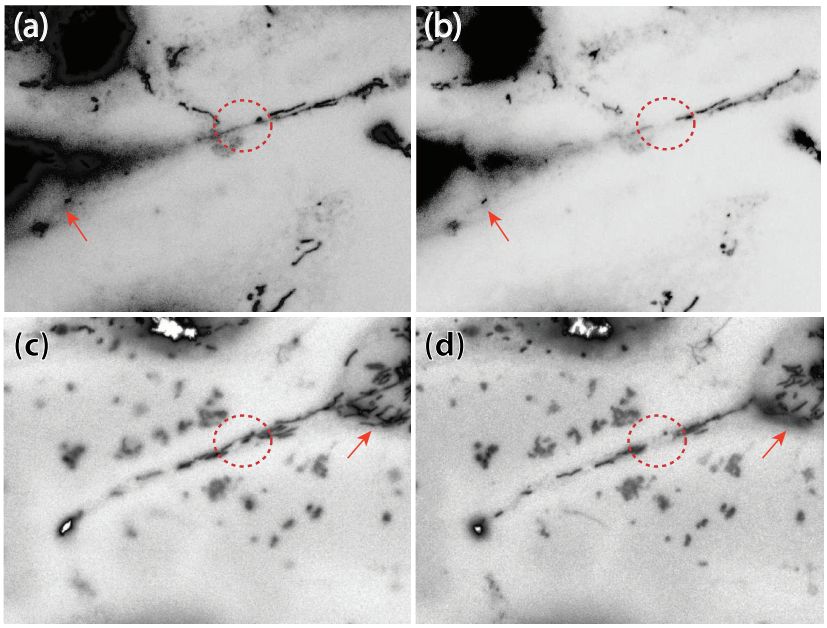

Figure 3.12: (a) and (c) before; (b) and (d) after femtosecond ablation of individual mitochondria stained with Mitotracker Red 580; 4.08 MHz, 240-fs, 2 nJ. Red arrows indicate the cell bodies.

Consequently, the system's capacity of targeting an individual organelle inside a single, live SaOS-2 cells are investigated using the 100X objective. We make a partial ablation of an individual mitochondrion, which is stained with Mitotracker Red 580, employing 2 nJ pulses (Figure 3.12). The possibility of photobleaching instead of an actual ablation is ruled out by applying the Fluorescence Recovery After Photobleach (FRAP) protocol for more than few hours after the nanosurgery operation. Constant observation of the operated cell after the femtosecond nanosurgery indicates that the cell viability was not intervened.

Finally, we employ the nanosurgery system to perform axotomy on a single, differentiated neuroendocrine PC12 cell. The axon of a PC12 cell is dissected with the incident laser beam with 8 nJ pulse energy at 32.7 MHz repetition rate (Figure 3.13). In this case, the operation interferes with the survival of the operated cell and after several minutes, symptoms of Wallerian Degeneration occurs, characteristic with the formation of the repeated bead-like structures along the axon.

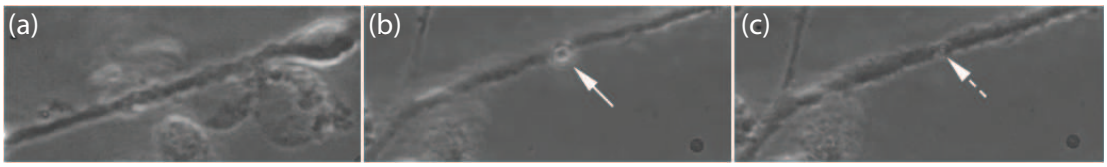

Figure 3.13: (a) Before and (b) at the moment of laser axotomy (white arrow indicates the incident laser beam on the axon). (c) After axotomy (white dashed arrow indicates the micro-damage); 32.7 MHz, 240-fs, 8 nJ.

3.5 Conclusion

In conclusion, in this part of this thesis study, we develop an ultrashort pulse fiber laser-microscope integrated system and demonstrate its biophotonic application for nanosurgery. The system comprises a novel and highly feasible assembly for ultrashort-pulsed sub-cellular nanosurgery, taking maximal advantages fiber

technology. The laser setup is highly robust; with the use of custom-designed FPGA electronics functioning through fiber-coupled AOMs, it is possible to create pulse sequences with no limitations (apart from the max. repetition rate, which is that of the oscillator), while the MOPA design makes the individual pulse energies remain identical. Such benefits are achieved at a portion of the price of a titanium:sapphire laser, which has traditionally been utilised as the system of choice for such studies. This study that presents a notably low-cost and practical system will lead an increase in the employment of ultrashort-pulsed laser-based ablation studies in biological sciences.

Chapter 4

Summary and Outlook

As a part of this thesis study, we have demonstrated controlled surface modification of Ti6Al4V metal implants using pulsed fiber lasers delivering picosecond and femtosecond pulses. Comparison of the surface topographies generated with nanosecond pulses indicated the clear advantages of ultrashort pulses, those which minimizes thermal effects and increases topographical precision. In addition to that, for micron-scale surface modifications, we demonstrated that the picosecond pulses virtually offers a quality similar to those of femtosecond pulses. Because of the fact that picosecond systems does not require a grating compressor for further compression of the pulses, and the laser beam is directly delivered from the optical fiber, use of picosecond systems at MHz repetition rates offers great potential, especially for in vivo applications.

We demonstrated that, by altering the pulse energy, exposure time and the scanning pattern, a diverse range of surface textures can be created using both pico- and femtosecond regimes. We further showed that, for the generation of micrometer-sized surface textures, pico- and femtosecond regimes both yield similar results. On the other hand, femtosecond pulses at low fluence levels leads to nanoscale modification of the surfaces, which seems not to be possible in picosecond regime. Such data indicates that, even in the picosecond regime, the thermal effects might dominate the incident events and lead to deformation of the expected topographical features.

Next, we utilized spectroscopic techniques to establish a better understanding of the mechanisms behind modification of the sample surfaces. These results showed that oxygen is present in the modified regions, in contrast to non-modified (non-irradiated) regions. The amount of oxygen in modified regions seem to be in the same range for all pulse regimes. Further characterizations indicated that the main portion of this oxygen is accumulated at the irradiate region in the form of titanium dioxide, particularly in tetragonal rutile structure of TiO_2. Therefore, we conclude that, especially the protruding structures (textures those are higher from the original surface level) created by laser irradiation are largely composed of this rutile phase, irrespective of the operation in femto-, pico- or nanosecond regime.

Then, investigated the efficiency of laser-modificed surfaces in cellular adhesion and proliferation. We found that surfaces modified with picosecond pulses offers a cell attachment and proliferation quality as good as commercially produced surfaces, which are widely accepted to be surface modifications of choice for qualified tissue integration.

Furthermore, we presented the data for the clear tendency of cells to align with linear micro-topographies created by the picosecond laser, a phenomenon termed as topographical or contact guidance. On the other hand, there was no distinguishable alignment on the surfaces with nanometer-scale height differences created with femtosecond pulses, thus, there was no improvement in adhesion either, which might be an indication of inadequate interaction between the cells and the nanometer scale topographies.

We also observed the de-promotion of cell adhesion and proliferation. Our data indicated that, by employing surface structures that hinders or interferes with the biomechanics of cells at the biomaterial-tissue interface, cell attachment and spreading can also be altered in an antagonistic manner.

Considering the laser modification of biomaterial surfaces, a final word would be that the significant advantage of laser modification is its capacity to selectively treat different regions of an implant surface with different patterns, which may

be designed to enhance or inhibit cell attachment. Such spatial selectivity is definitely not possible with most of the conventional techniques such as mechanical and chemical methods. Although our emphasis has been on texturing of Ti-based dental implant surfaces, these results can easily be adapted to different materials and textures.

In the second part of this thesis study, we developed and made use of an ultrashort pulse fiber laser-microscope integrated system for sub-cellular nanosurgery. The custom-developed system is based on a mode-locked Yb-fiber oscillator, seeding a multi-stage fiber amplifier and incorporating a fiber-coupled AOM for repetition rate control, a diffraction grating compressor and a free-space AOM for pulse picking. This enables complete control over the pulse sequence pattern. The laser is coupled to a diffraction-limited fluorescence microscope, with computerized imaging and sample positioning.

Firstly, the integrated systems capability of performing femtosecond photodisruption of biological samples was tested on frozen sections of mouse gastrocnemius muscle tissue. With a beam diameter around 2.2 μm using the 20X objective, linear cuts with the line widths of same sizes were generated.

Next, we applied pulsed-laser ablations experiments on glutaraldehyde fixated osteosarcoma cell lines by using the 60X objective, which leads to sub-micron-sized ablation regions. This means that the size of a single ablated area is smaller than the size of the diffraction limited-beam, which is for our laser's wavelength around 1 μm. Such an observation is consistent with the expectations of nonlinear processes, most probably multiphoton processes, during the laser irradiation with femtosecond lasers.

Subsequently, laser ablation of a single organelle was experimented by using 100X objective. For these experiments we used mitochondria and accordingly we stained the mitochondria with organelle specific fluorescent dyes. We presented the data for femtosecond nanosurgery of single, individual organelles. Furthermore, we observed that even a portion of a single mitochondrion could be ablated. The possibility for photobleaching, which refers to the fluorescence loss instead of actual ablation via laser irradiation, was examined by applying FRAP

(Fluorescence Recovery After Photobleach) protocol for several hours after the nanosurgery. As a result, it was proven that the organelle disappearances after fs- laser irradiation were not only due to fluorescence loss but because of actual material removal, which means ablation. Subsequent monitoring of the operated cell indicated that the cell viability and cellular homeostasis was not influenced by ablation.

Finally, we have used our integrated nanosurgery system to dissect the axon of a differentiated neuroendocrine PC12 cells. The axon of a PC12 cell was damaged with the fs-laser pulses and it was observed that even a damage at the size of a few micrometers could result in the intervention of the viability of the neuron. This viability and homeostasis change was characterized with the formation of bead-like structures all along the operated axon, which is one of the distinctive indications of nerve damages and the whole process is called Wallerian Degeneration. On the other hand, even smaller pulse energies and pulse numbers should be tried to see if there is any adjustable level that will not cause such an homeostatic imbalance. In any type of the nanosurgery applications we have presented by now, are in the range of few or several nanojules of pulse energies.

Nonlinear biophotonics or ultrashort-pulsed biophotonics is a novel research area and offers a potential for biological applications. Over the past decade, a number of proof-of-principle study demonstrated that such a methodology is extremely efficient and provides an exceptional control both on spatial and temporal domains. In addition to those proof-of-concept studies, publications utiilizing this methodology as an experimental tool have begun to accumulate in the scientific literature as well. Thereby it seems that, especially by taking the above-mentioned advantages of fiber lasers, the diversity of applications of ultrashort-pulsed biophotonics will continue to develop in further different directions, in addition to the fact that biologists will further adopt this methodology as a routine technique for their laboratories.

4.1 Near-Future Perspectives

"*Understanding the human brain is one of the greatest challenges facing 21st century science. If we can rise to the challenge, we can gain fundamental insights into what it means to be human, develop new treatments for brain diseases...*"

This is the first paragraph of the report submitted to the European Commission by The Human Brain Project consortium in 2013. To achieve this aim and to unravel the functional brain-map, being capable of triggering the firing of neurons in a controlled manner in the awake animal in a rapid way is the most critical challenge. Although conventional electrophysiology methods that measure neural activity to decipher neuronal network operations exist, combinatorial use of optics and genetic labeling methods is currently rather promising for neuro-circuit analysis and brain mapping.

It seems plausible that, as articulated elegantly by Francis Crick articulated in 1999, "*the ideal signal would be light, probably at an infrared wavelength to allow the light to penetrate far enough. This seems rather far-fetched but it is conceivable that molecular biologists could engineer a particular cell type to be sensitive to light in this way*" [103].

Today, this idea is not that "far-fetched; particularly, advances on microscopic and fiber-optic techniques have made considerable progress in that direction. A striking novel methodology is optogenetics, which utilizes light to control neuronal activity that have been genetically modified to respond to light. Optogenetics, which in 2010, was selected as the method of the year by Nature Methods, is a neuromodulation method intensely used in neuroscience that makes the combinatory use of techniques from optics and genetics to monitor and manipulate the activity of individual neurons [104].

The interrelated advancements both in biological and photonic technologies lead to the increasing combination of the tools and methodologies of these disciplines. An active example is the case is that optical fibers have found considerable usage in biological imaging, particularly in neuroscience, in parallel to the

the progresses in optogenetics [105] (Figure 4.1). Fiber-optic light delivery and collection systems are particularly advantageous for studies on freely behaving animals, mainly due to the fact that it eliminates the use of an objective lens, hence, readily reaching deep tissue locations with a minimal invasion [106].

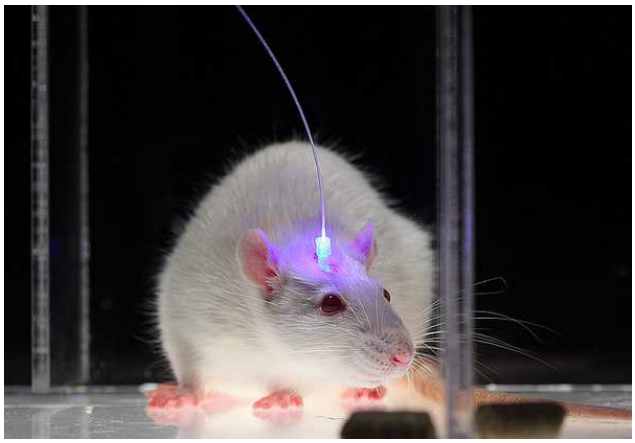

Figure 4.1: The conventional form of in vivo optogenetics mounting fiber-optic cables in the rodent head. [107]

Moreover, it was recently reported that the significant scattering and absorption of the incident light resulting in lower penetration beneath tissues, can be further eliminated by combining the flexible nature of fiber-optic components with the two-photon absorption phenomena [108]. With the demonstration of the fiber-optic two-photon near-infrared optogenetic stimulation, the articulations of Francis Crick are almost completely realized after nearly 15 years.

In parallel to these developments, other exciting and promising developments has also occurred in the field of neurobiophotonics that eliminates the major drawback of optogenetics, which is the necessity of transgenesis that allows the neurons respond to light. The obligation of transgenesis protocol in optogenetics makes it inapplicable for human studies and requires a complicated series processes of introducing an exogenous gene into the living organism. Recent researches demonstrating the direct optical stimulation of excitable cells would pave the way for analyzing the neuronal networks without intervening the natural, wild-type conditions of living organisms. A remarkable study that utilizes

pulsed lasers for such non-invasive stimulation of both neuronal and cardiac tissue is considerably promotive [109]. Furthermore, the employment of ultrashort pulses for nonlinear stimulation, hence that would result in higher penetration depth and more precise stimulation, is notably promising [110].

Finally, taking into account the neuronal nanosurgery results that we have reported in this thesis study, it can immediately be speculated that, as a parallel operation to the neuronal network analysis as referred in the paragraph above, the further manipulation and engineering of the network via "laser-tailoring" would be an unprecedented methodology.

However, these advancements only represent the progress in methodologies and practical tools required for the achievement of the main goal, which is the comprehensive understanding of how the brain works; therefor, the final challenge will be the development of the "Brain Theory". Nevertheless, such progression indicates that the 21st century science, especially biophotonics, is stepping towards the ultimate goal. When such developments in biophotonics makes an ideal combination with nanotechnology, the flawless exploitation of the non-invasive nature of light will be truly realized.

Bibliography

[1] W. R. Zipfel, R. M. Williams, and W. W. Webb, "Nonlinear magic: multiphoton microscopy in the biosciences," *Nature biotechnology*, vol. 21, no. 11, pp. 1369–1377, 2003.

[2] N. P. Rougier, "Scientific illustrations."

[3] Y. Shen, C. S. Friend, Y. Jiang, D. Jakubczyk, J. Swiatkiewicz, and P. N. Prasad, "Nanophotonics: interactions, materials, and applications," *The Journal of Physical Chemistry B*, vol. 104, no. 32, pp. 7577–7587, 2000.

[4] P. N. Prasad, *Introduction to biophotonics*. John Wiley & Sons, 2004.

[5] M. Khajavikhan, A. Simic, M. Katz, J. Lee, B. Slutsky, A. Mizrahi, V. Lomakin, and Y. Fainman, "Thresholdless nanoscale coaxial lasers," *Nature*, vol. 482, no. 7384, pp. 204–207, 2012.

[6] W. Cai, A. P. Vasudev, and M. L. Brongersma, "Electrically controlled nonlinear generation of light with plasmonics," *Science*, vol. 333, no. 6050, pp. 1720–1723, 2011.

[7] B. Öktem, I. Pavlov, S. Ilday, H. Kalaycıoğlu, A. Rybak, S. Yavaş, M. Erdoğan, and F. Ö. Ilday, "Nonlinear laser lithography for indefinitely large-area nanostructuring with femtosecond pulses," *Nature Photonics*, vol. 7, no. 11, pp. 897–901, 2013.

[8] M. D. Hutchinson, F. C. Garcia, J. E. Mandel, N. Elkassabany, E. S. Zado, M. P. Riley, J. M. Cooper, R. Bala, D. S. Frankel, D. Lin, *et al.*, "Efforts

to enhance catheter stability improve atrial fibrillation ablation outcome," *Heart Rhythm*, vol. 10, no. 3, pp. 347–353, 2013.

[9] J. Sohier, I. Carubelli, P. Sarathchandra, N. Latif, A. H. Chester, and M. H. Yacoub, "The potential of anisotropic matrices as substrate for heart valve engineering," *Biomaterials*, vol. 35, no. 6, pp. 1833–1844, 2014.

[10] J. C. Fricain, S. Schlaubitz, C. Le Visage, I. Arnault, S. M. Derkaoui, R. Siadous, S. Catros, C. Lalande, R. Bareille, M. Renard, *et al.*, "A nano-hydroxyapatite–pullulan/dextran polysaccharide composite macroporous material for bone tissue engineering," *Biomaterials*, vol. 34, no. 12, pp. 2947–2959, 2013.

[11] S. Tarafder, N. M. Davies, A. Bandyopadhyay, and S. Bose, "3d printed tricalcium phosphate bone tissue engineering scaffolds: effect of sro and mgo doping on in vivo osteogenesis in a rat distal femoral defect model," *Biomaterials Science*, vol. 1, no. 12, pp. 1250–1259, 2013.

[12] D. Williams, "Tissue-biomaterial interactions," *Journal of Materials science*, vol. 22, no. 10, pp. 3421–3445, 1987.

[13] J. M. Anderson, A. Rodriguez, and D. T. Chang, "Foreign body reaction to biomaterials," in *Seminars in immunology*, vol. 20, pp. 86–100, Elsevier, 2008.

[14] J. D. Bryers, C. M. Giachelli, and B. D. Ratner, "Engineering biomaterials to integrate and heal: the biocompatibility paradigm shifts," *Biotechnology and bioengineering*, vol. 109, no. 8, pp. 1898–1911, 2012.

[15] D. Williams, "General concepts of biocompatibility," in *Handbook of biomaterial properties*, pp. 481–489, Springer, 1998.

[16] Y. Onuki, U. Bhardwaj, F. Papadimitrakopoulos, and D. J. Burgess, "A review of the biocompatibility of implantable devices: current challenges to overcome foreign body response," *Journal of diabetes science and technology*, vol. 2, no. 6, pp. 1003–1015, 2008.

[17] D. F. Williams, "On the mechanisms of biocompatibility," *Biomaterials*, vol. 29, no. 20, pp. 2941–2953, 2008.

[18] B. Kasemo and J. Lausmaa, "Material-tissue interfaces: the role of surface properties and processes.," *Environmental health perspectives*, vol. 102, no. Suppl 5, p. 41, 1994.

[19] B. Kasemo and J. Lausmaa, "Surface science aspects on inorganic biomaterials," *CRC Crit. Rev. Clin. Neurobiol.;(United States)*, vol. 4, 1986.

[20] B. Kasemo and J. Lausmaa, "Biomaterials from a surface science perspective," *Surface Characterization of Biomaterials, Elsevier, New York*, pp. 1–12, 1988.

[21] J. Woodman, J. Jacobs, J. Galante, and R. Urban, "Metal ion release from titanium-based prosthetic segmental replacements of long bones in baboons: A long-term study," *Journal of Orthopaedic Research*, vol. 1, no. 4, pp. 421–430, 1983.

[22] J. Jacobs, A. Skipor, J. Black, R. Urban, and J. Galante, "Release and excretion of metal in patients who have a total hip-replacement component made of titanium-base alloy," *J Bone Joint Surg Am*, vol. 73, no. 10, pp. 1475–86, 1991.

[23] D. M. Brunette, *Titanium in medicine: material science, surface science, engineering, biological responses, and medical applications*. Springer, 2001.

[24] J.-L. Dewez, A. Doren, Y.-J. Schneider, and P. G. Rouxhet, "Competitive adsorption of proteins: key of the relationship between substratum surface properties and adhesion of epithelial cells," *Biomaterials*, vol. 20, no. 6, pp. 547–559, 1999.

[25] I. Lynch, I. A. Blute, B. Zhmud, P. MacArtain, M. Tosetto, L. T. Allen, H. J. Byrne, G. F. Farrell, A. K. Keenan, W. M. Gallagher, *et al.*, "Correlation of the adhesive properties of cells to n-isopropylacrylamide/n-tert-butylacrylamide copolymer surfaces with changes in surface structure using contact angle measurements, molecular simulations, and raman spectroscopy," *Chemistry of materials*, vol. 17, no. 15, pp. 3889–3898, 2005.

[26] L. T. Allen, E. J. Fox, I. Blute, Z. D. Kelly, Y. Rochev, A. K. Keenan, K. A. Dawson, and W. M. Gallagher, "Interaction of soft condensed materials with living cells: phenotype/transcriptome correlations for the hydrophobic effect," *Proceedings of the National Academy of Sciences*, vol. 100, no. 11, pp. 6331–6336, 2003.

[27] M. J. Dalby, S. J. Yarwood, M. O. Riehle, H. J. Johnstone, S. Affrossman, and A. S. Curtis, "Increasing fibroblast response to materials using nanotopography: morphological and genetic measurements of cell response to 13-nm-high polymer demixed islands," *Experimental cell research*, vol. 276, no. 1, pp. 1–9, 2002.

[28] M. J. Dalby, M. O. Riehle, S. J. Yarwood, C. D. Wilkinson, and A. S. Curtis, "Nucleus alignment and cell signaling in fibroblasts: response to a micro-grooved topography," *Experimental cell research*, vol. 284, no. 2, pp. 272–280, 2003.

[29] T. Dvir, B. P. Timko, D. S. Kohane, and R. Langer, "Nanotechnological strategies for engineering complex tissues," *Nature nanotechnology*, vol. 6, no. 1, pp. 13–22, 2011.

[30] A. I. Teixeira, G. A. Abrams, P. J. Bertics, C. J. Murphy, and P. F. Nealey, "Epithelial contact guidance on well-defined micro-and nanostructured substrates," *Journal of cell science*, vol. 116, no. 10, pp. 1881–1892, 2003.

[31] C. J. Bettinger, R. Langer, and J. T. Borenstein, "Engineering substrate topography at the micro-and nanoscale to control cell function," *Angewandte Chemie International Edition*, vol. 48, no. 30, pp. 5406–5415, 2009.

[32] M. J. Dalby, N. Gadegaard, R. Tare, A. Andar, M. O. Riehle, P. Herzyk, C. D. Wilkinson, and R. O. Oreffo, "The control of human mesenchymal cell differentiation using nanoscale symmetry and disorder," *Nature materials*, vol. 6, no. 12, pp. 997–1003, 2007.

[33] T. K. Monsees, K. Barth, S. Tippelt, K. Heidel, A. Gorbunov, W. Pompe, and R. H. Funk, "Effects of different titanium alloys and nanosize surface

patterning on adhesion, differentiation, and orientation of osteoblast-like cells," *Cells Tissues Organs*, vol. 180, no. 2, pp. 81–95, 2005.

[34] E.-J. Chang, H.-H. Kim, J.-E. Huh, I. Kim, J. Seung Ko, C.-P. Chung, and H.-M. Kim, "Low proliferation and high apoptosis of osteoblastic cells on hydrophobic surface are associated with defective ras signaling," *Experimental cell research*, vol. 303, no. 1, pp. 197–206, 2005.

[35] M. J. Glimcher, "Molecular biology of mineralized tissues with particular reference to bone," *Reviews of Modern Physics*, vol. 31, no. 2, p. 359, 1959.

[36] A. L. Boskey and R. Mendelsohn, "Infrared spectroscopic characterization of mineralized tissues," *Vibrational Spectroscopy*, vol. 38, no. 1, pp. 107–114, 2005.

[37] C. Brighton, "Principles of fracture healing," *Instructional course lectures*, vol. 33, pp. 60–82, 1984.

[38] C. Stanford, J. Keller, and M. Solursh, "Bone cell expression on titanium surfaces is altered by sterilization treatments," *Journal of dental research*, vol. 73, no. 5, pp. 1061–1071, 1994.

[39] R. Branemark, P. Branemark, B. Rydevik, and R. R. Myers, "Osseointegration in skeletal reconstruction and rehabilitation: a review," *Journal of rehabilitation research and development*, vol. 38, no. 2, pp. 175–182, 2001.

[40] P.-I. Branemark, "Osseointegration and its experimental background," *The Journal of prosthetic dentistry*, vol. 50, no. 3, pp. 399–410, 1983.

[41] U. Meyer, U. Joos, J. Mythili, T. Stamm, A. Hohoff, T. Fillies, U. Stratmann, and H. Wiesmann, "Ultrastructural characterization of the implant/bone interface of immediately loaded dental implants," *Biomaterials*, vol. 25, no. 10, pp. 1959–1967, 2004.

[42] M. Franchi, M. Fini, D. Martini, E. Orsini, L. Leonardi, A. Ruggeri, G. Giavaresi, and V. Ottani, "Biological fixation of endosseous implants," *Micron*, vol. 36, no. 7, pp. 665–671, 2005.

[43] J. B. Park, "The biomedical engineering handbook," *Boca Raton, FL: CRC Press*, vol. 4, pp. 1–8, 2000.

[44] J. Y. Park and J. E. Davies, "Red blood cell and platelet interactions with titanium implant surfaces," *Clinical oral implants research*, vol. 11, no. 6, pp. 530–539, 2000.

[45] P. Roach, D. Eglin, K. Rohde, and C. C. Perry, "Modern biomaterials: a reviewbulk properties and implications of surface modifications," *Journal of Materials Science: Materials in Medicine*, vol. 18, no. 7, pp. 1263–1277, 2007.

[46] A. Curtis and C. Wilkinson, "Topographical control of cells," *Biomaterials*, vol. 18, no. 24, pp. 1573–1583, 1997.

[47] X. Liu, P. K. Chu, and C. Ding, "Surface modification of titanium, titanium alloys, and related materials for biomedical applications," *Materials Science and Engineering: R: Reports*, vol. 47, no. 3, pp. 49–121, 2004.

[48] C. Momma, S. Nolte, B. N Chichkov, A. Tünnermann, *et al.*, "Precise laser ablation with ultrashort pulses," *Applied surface science*, vol. 109, pp. 15–19, 1997.

[49] A. Y. Vorobyev and C. Guo, "Femtosecond laser nanostructuring of metals," *Optics express*, vol. 14, no. 6, pp. 2164–2169, 2006.

[50] M. Erdoğan, B. Öktem, H. Kalaycıoğlu, S. Yavaş, P. K. Mukhopadhyay, K. Eken, K. Özgören, Y. Aykaç, U. H. Tazebay, and F. Ö. Ilday, "Texturing of titanium (ti6al4v) medical implant surfaces with mhz-repetition-rate femtosecond and picosecond yb-doped fiber lasers," *Optics express*, vol. 19, no. 11, pp. 10986–10996, 2011.

[51] A. Chong, J. Buckley, W. Renninger, and F. Wise, "All-normal-dispersion femtosecond fiber laser," *Optics Express*, vol. 14, no. 21, pp. 10095–10100, 2006.

[52] F. Ilday, J. Buckley, W. Clark, and F. Wise, "Self-similar evolution of parabolic pulses in a laser," *Physical review letters*, vol. 92, no. 21, p. 213902, 2004.

[53] P. K. Mukhopadhyay, K. Ozgoren, I. L. Budunoglu, and O. Ilday, "All-fiber low-noise high-power femtosecond yb-fiber amplifier system seeded by an all-normal dispersion fiber oscillator," *Selected Topics in Quantum Electronics, IEEE Journal of*, vol. 15, no. 1, pp. 145–152, 2009.

[54] H. Kalaycioglu, B. Oktem, Ç. Şenel, P. Paltani, and F. Ilday, "Microjoule-energy, 1 mhz repetition rate pulses from all-fiber-integrated nonlinear chirped-pulse amplifier," *Optics letters*, vol. 35, no. 7, pp. 959–961, 2010.

[55] Y. Kathuria, "Laser microprocessing of metallic stent for medical therapy," *Journal of materials processing technology*, vol. 170, no. 3, pp. 545–550, 2005.

[56] K. Weman, *Welding processes handbook*. Elsevier, 2011.

[57] I. Etsion, "Improving tribological performance of mechanical components by laser surface texturing," *Tribology Letters*, vol. 17, no. 4, pp. 733–737, 2004.

[58] S. Porto, P. Fleury, and T. Damen, "Raman spectra of ti o 2, mg f 2, zn f 2, fe f 2, and mn f 2," *Physical Review*, vol. 154, no. 2, p. 522, 1967.

[59] H. Ma, J. Yang, Y. Dai, Y. Zhang, B. Lu, and G. Ma, "Raman study of phase transformation of tio¡ sub¿ 2¡/sub¿ rutile single crystal irradiated by infrared femtosecond laser," *Applied surface science*, vol. 253, no. 18, pp. 7497–7500, 2007.

[60] D. Buser, T. Nydegger, T. Oxland, D. L. Cochran, R. K. Schenk, H. P. Hirt, D. Snétivy, and L.-P. Nolte, "Interface shear strength of titanium implants with a sandblasted and acid-etched surface: A biomechanical study in the maxilla of miniature pigs," *Journal of biomedical materials research*, vol. 45, no. 2, pp. 75–83, 1999.

[61] D. Y. Sullivan, R. L. Sherwood, and T. N. Mai, "Preliminary results of a multicenter study evaluating a chemically enhanced surface for machined commercially pure titanium implants," *The Journal of prosthetic dentistry*, vol. 78, no. 4, pp. 379–386, 1997.

[62] M. F. Yanik, H. Cinar, H. N. Cinar, A. D. Chisholm, Y. Jin, and A. Ben-Yakar, "Neurosurgery: functional regeneration after laser axotomy," *Nature*, vol. 432, no. 7019, pp. 822–822, 2004.

[63] L. Sacconi, R. P. OConnor, A. Jasaitis, A. Masi, M. Buffelli, and F. S. Pavone, "In vivo multiphoton nanosurgery on cortical neurons," *Journal of biomedical optics*, vol. 12, no. 5, pp. 050502–050502, 2007.

[64] W. Watanabe, S. Matsunaga, T. Shimada, T. Higashi, K. Fukui, and K. Itoh, "Femtosecond laser disruption of mitochondria in living cells," *Medical Laser Application*, vol. 20, no. 3, pp. 185–191, 2005.

[65] J. Colombelli, E. G. Reynaud, and E. H. Stelzer, "Investigating relaxation processes in cells and developing organisms: from cell ablation to cytoskeleton nanosurgery," *Methods in cell biology*, vol. 82, pp. 267–291, 2007.

[66] R. Steiner, "Laser-tissue interactions," in *Laser and IPL Technology in Dermatology and Aesthetic Medicine*, pp. 23–36, Springer, 2011.

[67] R. R. Anderson and J. A. Parrish, "The optics of human skin," *Journal of Investigative Dermatology*, vol. 77, no. 1, pp. 13–19, 1981.

[68] R. M. Herd, J. S. Dover, K. A. Arndt, *et al.*, "Basic laser principles," *Dermatologic clinics*, vol. 15, no. 3, pp. 355–372, 1997.

[69] M. H. Niemz, *Laser-tissue interactions: fundamentals and applications*. Springer, 2007.

[70] I. Maxwell, *Application of femtosecond lasers for subcellular nanosurgery*. PhD thesis, Harvard University Cambridge, Massachusetts, 2006.

[71] E. L. Tanzi, J. R. Lupton, and T. S. Alster, "Lasers in dermatology: four decades of progress," *Journal of the American Academy of Dermatology*, vol. 49, no. 1, pp. 1–34, 2003.

[72] V. Venugopalan, A. Guerra III, K. Nahen, and A. Vogel, "Role of laser-induced plasma formation in pulsed cellular microsurgery and micromanipulation," *Physical review letters*, vol. 88, no. 7, p. 078103, 2002.

[73] A. Vogel and V. Venugopalan, "Mechanisms of pulsed laser ablation of biological tissues," *Chemical reviews*, vol. 103, no. 2, pp. 577–644, 2003.

[74] A. Vogel, J. Noack, G. Hüttman, and G. Paltauf, "Mechanisms of femtosecond laser nanosurgery of cells and tissues," *Applied Physics B*, vol. 81, no. 8, pp. 1015–1047, 2005.

[75] C. Sacchi, "Laser-induced electric breakdown in water," *JOSA B*, vol. 8, no. 2, pp. 337–345, 1991.

[76] D. N. Nikogosyan, A. A. Oraevsky, and V. I. Rupasov, "Two-photon ionization and dissociation of liquid water by powerful laser uv radiation," *Chemical Physics*, vol. 77, no. 1, pp. 131–143, 1983.

[77] L. Keldysh, "Ionization in the field of a strong electromagnetic wave," *Sov. Phys. JETP*, vol. 20, no. 5, pp. 1307–1314, 1965.

[78] U. K. Tirlapur, K. König, C. Peuckert, R. Krieg, and K.-J. Halbhuber, "Femtosecond near-infrared laser pulses elicit generation of reactive oxygen species in mammalian cells leading to apoptosis-like death," *Experimental cell research*, vol. 263, no. 1, pp. 88–97, 2001.

[79] R. F. Steinert and C. A. Puliafito, *The Nd-YAG laser in ophthalmology: principles and clinical applications of photodisruption*. Saunders Philadelphia, 1985.

[80] I. Ratkay-Traub, I. E. Ferincz, T. Juhasz, R. M. Kurtz, and R. R. Krueger, "First clinical results with the femtosecond neodynium-glass laser in refractive surgery.," *Journal of refractive surgery (Thorofare, NJ: 1995)*, vol. 19, no. 2, pp. 94–103, 2002.

[81] C. B. Schaffer, A. Brodeur, J. F. García, and E. Mazur, "Micromachining bulk glass by use of femtosecond laser pulses with nanojoule energy," *Optics letters*, vol. 26, no. 2, pp. 93–95, 2001.

[82] W. Denk, J. H. Strickler, W. W. Webb, *et al.*, "Two-photon laser scanning fluorescence microscopy," *Science*, vol. 248, no. 4951, pp. 73–76, 1990.

[83] K. Itoh, W. Watanabe, and Y. Ozeki, "Nonlinear ultrafast focal-point optics for microscopic imaging, manipulation, and machining," *Proceedings of the IEEE*, vol. 97, no. 6, pp. 1011–1030, 2009.

[84] E. Botvinick, V. Venugopalan, J. Shah, L. Liaw, and M. Berns, "Controlled ablation of microtubules using a picosecond laser," *Biophysical journal*, vol. 87, no. 6, pp. 4203–4212, 2004.

[85] G. J. Tserevelakis, S. Psycharakis, B. Resan, F. Brunner, E. Gavgiotaki, K. Weingarten, and G. Filippidis, "Femtosecond laser nanosurgery of subcellular structures in hela cells by employing third harmonic generation imaging modality as diagnostic tool," *Journal of biophotonics*, vol. 5, no. 2, pp. 200–207, 2012.

[86] K. Rhodes, I. Clark, M. Zatcoff, T. Eustaquio, K. L. Hoyte, and M. R. Koller, "Cellular laserfection," *Methods in cell biology*, vol. 82, pp. 309–333, 2007.

[87] K. König, I. Riemann, P. Fischer, and K. Halbhuber, "Intracellular nanosurgery with near infrared femtosecond laser pulses.," *Cellular and molecular biology (Noisy-le-Grand, France)*, vol. 45, no. 2, pp. 195–201, 1999.

[88] M. Stiess, N. Maghelli, L. C. Kapitein, S. Gomis-Rüth, M. Wilsch-Bräuninger, C. C. Hoogenraad, I. M. Tolić-Nørrelykke, and F. Bradke, "Axon extension occurs independently of centrosomal microtubule nucleation," *Science*, vol. 327, no. 5966, pp. 704–707, 2010.

[89] C. Tängemo, P. Ronchi, J. Colombelli, U. Haselmann, J. C. Simpson, C. Antony, E. H. Stelzer, R. Pepperkok, and E. G. Reynaud, "A novel laser nanosurgery approach supports de novo golgi biogenesis in mammalian cells," *Journal of cell science*, vol. 124, no. 6, pp. 978–987, 2011.

[90] T. Higaki, N. Kutsuna, Y. Hosokawa, K. Akita, K. Ebine, T. Ueda, N. Kondo, and S. Hasezawa, "Statistical organelle dissection of arabidopsis guard cells using image database lips," *Scientific reports*, vol. 2, 2012.

[91] N. Shen, D. Datta, C. B. Schaffer, P. LeDuc, D. E. Ingber, and E. Mazur, "Ablation of cytoskeletal filaments and mitochondria in live cells using a femtosecond laser nanoscissor," *Mech. Chem. Biosyst*, vol. 2, no. 1, pp. 17–25, 2005.

[92] N. Huda, S. Abe, L. Gu, M. S. Mendonca, S. Mohanty, and D. Gilley, "Recruitment of trf2 to laser-induced dna damage sites," *Free Radical Biology and Medicine*, vol. 53, no. 5, pp. 1192–1197, 2012.

[93] K. König, I. Riemann, and W. Fritzsche, "Nanodissection of human chromosomes with near-infrared femtosecond laser pulses," *Optics Letters*, vol. 26, no. 11, pp. 819–821, 2001.

[94] A. Csaki, F. Garwe, A. Steinbrück, G. Maubach, G. Festag, A. Weise, I. Riemann, K. König, and W. Fritzsche, "A parallel approach for subwavelength molecular surgery using gene-specific positioned metal nanoparticles as laser light antennas," *Nano letters*, vol. 7, no. 2, pp. 247–253, 2007.

[95] A. Villalobos, L. Gu, and S. Mohanty, "All-optical control of neuronal function via optical delivery of light-sensitive proteins and optogenetic stimulation," in *SPIE BiOS*, pp. 82076B–82076B, International Society for Optics and Photonics, 2012.

[96] M. Tsukakoshi, S. Kurata, Y. Nomiya, Y. Ikawa, and T. Kasuya, "A novel method of dna transfection by laser microbeam cell surgery," *Applied Physics B*, vol. 35, no. 3, pp. 135–140, 1984.

[97] K. Kuetemeyer, A. Lucas-Hahn, B. Petersen, H. Niemann, and A. Heisterkamp, "Femtosecond laser-induced fusion of nonadherent cells and two-cell porcine embryos," *Journal of biomedical optics*, vol. 16, no. 8, pp. 088001–088001, 2011.

[98] M. Oren-Suissa and B. Podbilewicz, "Cell fusion during development," *Trends in cell biology*, vol. 17, no. 11, pp. 537–546, 2007.

[99] R. W. Steubing, S. Cheng, W. H. Wright, Y. Numajiri, and M. W. Berns, "Laser induced cell fusion in combination with optical tweezers: the laser cell fusion trap," *Cytometry*, vol. 12, no. 6, pp. 505–510, 1991.

[100] R. L. Fork, "Laser stimulation of nerve cells in aplysia," *Science*, vol. 171, no. 3974, pp. 907–908, 1971.

[101] X. Liu, X. Lv, S. Zeng, W. Zhou, and Q. Luo, "Noncontact and nondestructive identification of neural circuits with a femtosecond laser," *Applied Physics Letters*, vol. 94, no. 6, p. 061113, 2009.

[102] Ö. Ilday, H. Lim, J. Buckley, F. Wise, *et al.*, "Practical all-fiber source of high-power, 120-fs pulses at 1 μm," *Optics letters*, vol. 28, no. 15, pp. 1362–1364, 2003.

[103] F. Crick, "The impact of molecular biology on neuroscience," *Philosophical Transactions of the Royal Society of London. Series B: Biological Sciences*, vol. 354, no. 1392, pp. 2021–2025, 1999.

[104] K. Deisseroth, G. Feng, A. K. Majewska, G. Miesenböck, A. Ting, and M. J. Schnitzer, "Next-generation optical technologies for illuminating genetically targeted brain circuits," *The Journal of Neuroscience*, vol. 26, no. 41, pp. 10380–10386, 2006.

[105] B. A. Wilt, L. D. Burns, E. T. W. Ho, K. K. Ghosh, E. A. Mukamel, and M. J. Schnitzer, "Advances in light microscopy for neuroscience," *Annual review of neuroscience*, vol. 32, p. 435, 2009.

[106] T. Knopfel and E. S. Boyden, *Optogenetics: Tools for Controlling and Monitoring Neuronal Activity*, vol. 196. Elsevier, 2012.

[107] Editorial, "Method of the year 2010," *Nature Methods*, vol. 8, no. 1, pp. 1–1, 2011.

[108] K. Dhakal, L. Gu, B. Black, and S. Mohanty, "Fiber-optic two-photon optogenetic stimulation," *Optics letters*, vol. 38, no. 11, pp. 1927–1929, 2013.

[109] M. W. Jenkins, A. R. Duke, S. Gu, Y. Doughman, H. Chiel, H. Fujioka, M. Watanabe, E. Jansen, and A. Rollins, "Optical pacing of the embryonic heart," *Nature photonics*, vol. 4, no. 9, pp. 623–626, 2010.

[110] C. Hosokawa, Y. Sakamoto, S. N. Kudoh, Y. Hosokawa, and T. Taguchi, "Femtosecond laser-induced stimulation of a single neuron in a neuronal network," *Applied Physics A*, vol. 110, no. 3, pp. 607–612, 2013.